European Journal of Medicinal Chemistry 265 (2024) 116063

Contents lists available at ScienceDirect

European Journal of Medicinal Chemistry

journal homepage: www.elsevier.com/locate/ejmech

Research paper

Identification of 4-amino-2-Pyridones as new potent PCSK9 inhibitors: From phenotypic hit discovery to *in vivo* tolerability

Lisa Giannessi [a,1], Maria Giovanna Lupo [b,1], Ilaria Rossi [c], Maria Grazia Martina [a], Antonietta Vilella [d], Martina Bodria [d], Daniela Giuliani [d], Francesca Zimetti [a], Ilaria Zanotti [a], Francesco Potì [e], Franco Bernini [a], Nicola Ferri [b,f,**], Marco Radi [a,*]

[a] Dipartimento di Scienze Degli Alimenti e Del Farmaco (DipALIFAR), Università Degli Studi di Parma, Viale Delle Scienze, 27/A, 43124, Parma, Italy
[b] Department of Medicine, University of Padova, 35128, Padova, Italy
[c] Department of Pharmaceutical and Pharmacological Sciences, University of Padova, 351131, Padova, Italy
[d] Department of Biomedical, Metabolic and Neural Sciences, University of Modena and Reggio Emilia, 41125, Modena, Italy
[e] Department of Medicine and Surgery, Unit of Neuroscience, University of Parma, 43125, Parma, Italy
[f] Veneto Institute of Molecular Medicine, Padua, 35129, Italy

ARTICLE INFO

Keywords:
PCSK9
Small molecules
Pyridones
Phenotypic drug discovery

ABSTRACT

Among the strategies to overcome the underperformance of statins in cardiovascular diseases (CVDs), the development of drugs targeting the Proprotein Convertase Subtilisin-like Kexin type 9 (PCSK9) is considered one of the most promising. However, only anti-PCSK9 biological drugs have been approved to date, and orally available small-molecules for the treatment of hypercholesterolemic conditions are still missing on the market. In the present work, we describe the application of a phenotypic approach to the identification and optimization of 4-amino-2-pyridone derivatives as a new chemotype with anti-PCSK9 activity. Starting from an in-house collection of compounds, functional assays on HepG2 cells followed by a chemistry-driven hit optimization campaign, led to the potent anti-PCSK9 candidate **5c**. This compound, at 5 μM, totally blocked PCSK9 secretion from HepG2 cells, significantly increased LDL receptor (LDLR) expression, and acted cooperatively with simvastatin by reducing its induction of PCSK9 expression. Finally, compound **5c** also proved to be well tolerated in C57BL/6J mice at the tested concentration (40 mg/kg) with no sign of toxicity or behavior modifications.

1. Introduction

Proprotein Convertase Subtilisin/Kexin type 9 (PCSK9) represents the most effective pharmacological target for reducing low-density lipoprotein cholesterol (LDL-C) levels and cardiovascular diseases [1]. PCSK9 is mainly synthetized by the liver and can be detected in the circulation. Its expression depends on the transcriptional activities of the sterol regulatory element-binding protein 2 (SREBP2) and HNF1α factors. In the endoplasmic reticulum, the activity of PCSK9 catalytic domain is required for the self-cleavage. After autocleavage, the prodomain remains non-covalently bound to the catalytic domain, giving rise to the mature form of PCSK9, which is then secreted. Circulating PCSK9 binds to the LDL receptor (LDLR), driving its degradation by the lysosome, decreasing the hepatic cellular surface density of LDLRs, and consequently reducing the LDL uptake and increasing the circulating LDL-C levels [2,3].

PCSK9 is a well-validated target for hypercholesterolemia treatment and two monoclonal antibodies (mAb) alirocumab and evolocumab, and the small interfering RNA (siRNA) inclisiran represent the available pharmacological tools to inhibit its function. The efficacy of anti-PCSK9 mAbs may reach up to 55 % LDL-C lowering as monotherapy [4] and up to a 61 % when added to standard therapy [5,6]. Importantly, biological studies have also demonstrated that the most common hypocholesterolemic agents statins induce PCSK9 overexpression, contributing to the upset of statin resistance [7]. Hence, co-treatment with statins and PCSK9 inhibitors can further lower the risk of adverse cardiovascular events, acting cooperatively [8]. Nonetheless, the available anti-PCSK9 biological drugs present a few important drawbacks: 1) very high costs;

* Corresponding author. Dipartimento di Scienze degli Alimenti e del Farmaco, Università, degli Studi di Parma, Viale delle Scienze, 27/A, 43124, Parma, Italy.
** Corresponding author. Department of Medicine, University of Padova, 35131, Padova, Italy.
E-mail addresses: nicola.ferri@unipd.it (N. Ferri), marco.radi@unipr.it (M. Radi).
[1] These authors equally contributed to the present work.

https://doi.org/10.1016/j.ejmech.2023.116063
Received 9 June 2023; Received in revised form 15 December 2023; Accepted 15 December 2023
Available online 20 December 2023

2) administration by subcutaneous injection (poor compliance and convenience); 3) immunogenicity for long term treatments. On the other hand, the most recently approved siRNA inclisiran [9,10], could be less expensive than mAbs but still has some drawbacks, such as the long pharmacokinetic profile, the parenteral administration (the drug is administered by subcutaneous injection every 6 months) and a still undefined efficacy/safety profile [11]. More affordable orally bioavailable small-molecule drugs, able to modulate circulating level of PCSK9, are still missing on the market and represent a unique drug discovery opportunity.

In the last few years, different classes of small molecules have been reported in the literature as promising anti-PCSK9 drug candidates, acting through different mechanisms of action (Fig. 1) [12]. The knowledge of PCSK9 biochemical pathway has in fact allowed to target different steps of its life cycle with specific inhibitors, and both rational drug design and phenotypic screening approaches have led to the identification of promising candidates [13,14]. These small-molecule PCSK9 inhibitors can be broadly classified in two main categories: *i)* small-molecules directly binding PCSK9 (e.g. inhibitors of LDLR-PCSK9 interaction, such as the imidazole-based peptidomimetic developed by Silvani et al. [15,16], the guanidine derivative identified by Burgess et al. [17], or the very promising macrocyclic peptide MK016 [18,19]; cryptic groove inhibitors and allosteric inhibitors, such as the amino-thiazole derivative presented by Petrilli et al. [20]); and *ii)* small-molecules preventing PCSK9 synthesis by interaction with other molecular targets (e.g. transcription inhibitors, such as the xanthine derivatives developed by Wang and coworkers [21], or translation inhibitors, such as the piperidine derivative identified by Pfizer [22–25]) [26,27].

The most advanced in the clinical development is the macrocyclic peptide MK-0616, currently in phase 2, that expressed an exquisite potency and selectivity for PCSK9 [18,19]. Despite several small-molecule inhibitors have been patented and reported in the literature in the last few years, no candidates have been approved so far and the development of new PCSK9 inhibitors therefore remains a task of great interest for the medicinal chemistry community.

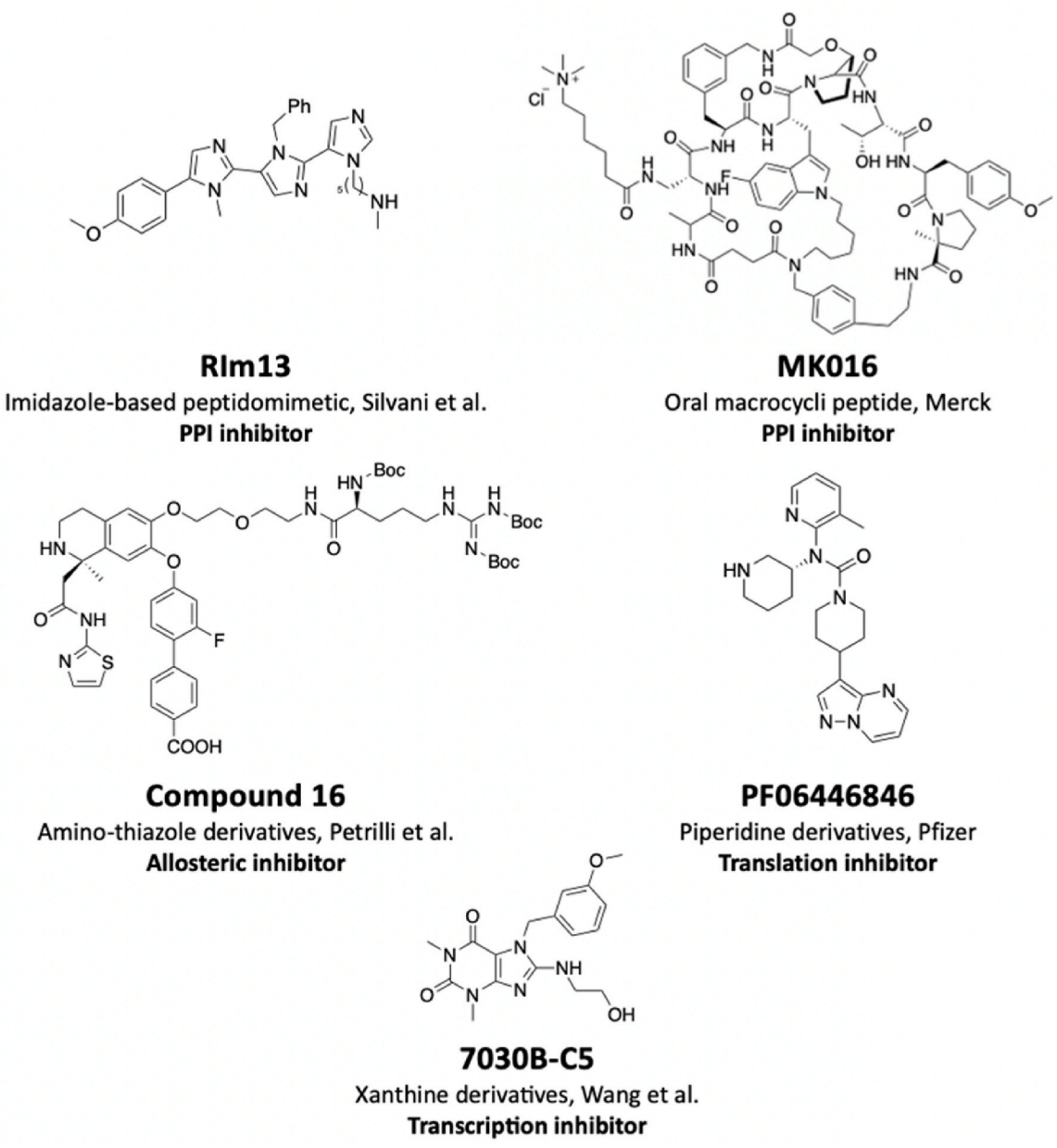

Fig. 1. Representative PCSK9 inhibitors.

In the present work, we describe our recent efforts in the identification of a new class of PCSK9 inhibitors endowed with a 2-pyridone scaffold and very promising *in vitro* anti-PCSK9 activity. After the identification of a hit compound through phenotypic screening of an in-house library of small molecules, a hit optimization campaign has been conducted by planning new closely related analogues that have been synthesized and biologically tested *in vitro*. Among the synthesized analogues, compound **5c** has been identified as the most promising candidate, showing complete block of PCSK9 secretion from HepG2 cells and significant induction of LDLR at 5 μM concentration, acting synergistically with simvastatin and resulting well tolerated in C57BL/6J mice.

2. Results and discussion

Despite the recent advancements in molecular and structural biology, predicting the specific molecular mechanisms of action of first-in-class drugs is still quite challenging and targeted drug development may lead to molecules unable to exert their effect on biological systems (e.g. cell, animal model) despite promising data on target engagement [28]. It is already well accepted that the application of a phenotypic drug-discovery approach is more effective in the identification of first-in-class drugs [29], and has already led to the discovery of promising PCSK9 inhibitors, as the naturally occurring compound berberine [30], the R-IMPP compound [31], and the 2,3′-diindolylmethane derivatives [32,33]. Recently, a methodical evaluation of target-based drug discovery's actual efficiency has been published, showing that just 9.4 % of authorized small-molecule drugs have been discovered using this strategy, evidencing the limitations of this approach [34]. We decided therefore to rely on a phenotypic approach to identify novel anti-PCSK9 agents, by screening a selection of 50 different chemotypes from our in-house collection of small molecules. An *in vitro* preliminary screening on human HepG2 cell system allowed to identify the 2-pyridone derivative **1** as the only hit compound able to reduce the expression of intracellular PCSK9 and its secretion after 24 h (h) incubation (Fig. 2). This 4-amino-2-pyridinone chemotype was previously investigated by our group as part of a targeted drug discovery campaign on new anticancer agents [35,36]. However, this class of molecules did not show the predicted anticancer activity *in vitro* and was further explored in the development of novel PCSK9 inhibitors. In the following experiments, compound **1** showed minor and not-significant reduction of cell viability on HepG2 cells after 24 h incubation at the highest tested concentrations (50–100 μM) (Fig. 2A). From this analysis, the effect of compound **1** on PCSK9 and other genes involved in lipid metabolism was assessed at the two lowest experimental concentrations, 6.25 and 12.5 μM respectively. PCSK9 expression was determined by Western blot analysis from total cell lysates (Fig. 2B and C) and PCSK9 secretion by ELISA assay from conditioned media (Fig. 2D). In our experimental condition, Simvastatin used as positive control, strongly induced the intracellular expression, as well as the secretion of PCSK9 (Fig. 2B, C, and 2D). Compound **1** almost completely abolished the protein expression of both proPCSK9 and mature PCSK9 at 12.5 μM, while no effect was observed at 6.25 μM compared to basal (Fig. 2B and C). The ELISA analysis of conditioned media showed a minor, albeit significant, reduction of PCSK9 at both tested concentrations (Fig. 2D). More in detail, at 12.5 μM, compound **1** reduced by 35.8 ± 5.8 % the extracellular amount of PCSK9 (Fig. 2D). To better investigate the molecular mechanism of action, we analyzed, by quantitative real-time PCR, the expression of PCSK9 mRNA and two key genes involved in the triglycerides and cholesterol biosynthesis: fatty-acid synthase (FAS) and hydroxy-methyl-glutaryl-CoA (HMG-CoA) reductase. Our results demonstrated that compound **1** specifically acts on PCSK9 mRNA by significantly and dose-dependently affecting its expression at concentrations of 6.25, 12.5 and 25 μM, without any effect on both FAS and HMG-CoA reductase (Fig. 2E, F and 2G). However, at higher concentrations (50 and 100 μM) compound **1** significantly affect also the expression of other genes regulated by SREBP2 pathway, such as HMG-CoA reductase but not those SREBP1-dependent, i.e., FAS (Fig. 2F and G). Thus, compound **1** showed a very effective and potent effect on PCSK9 expression that was more evident intracellularly than extracellularly. We hypothesized that this 4-amino-2-pyridone derivative may have a slow onset of action, that may thus result in an apparent discrepancy between intracellular and extracellular action, since PCSK9 secreted by the cells was affected by **1** for a restricted period of time compared to the action elicited at intracellular level. Regarding its potential molecular mechanism of action, compound **1** appeared to act by inhibiting PCSK9 gene transcription. The molecular target is still unknown, but both SREBP2 and HNF-1α are likely candidates, because of their well-established role in PCSK9 transcription's regulation [37–41]. The partial selectivity showed on PCSK9 transcription towards HMG-CoA reductase is difficult to explain. Analysis of PCSK9 promoter activity, revealed that compound **1** did not affect the basal activity but interferes with its activation by simvastatin (Fig. 2H). However, compound **1** was shown to activate the PCSK9 promoter activity only in the presence of a selective mutation of sterol responsive element (SRE) (Fig. 2I). Although the mechanism of action of this compound is still unknown, the data indicated a direct interference with the statin-activated SREBP pathway. Interestingly PCSK9 has been shown to be very responsive to statins compared to the LDL receptor [42], effect that may explain the partial selectivity of compound **1** on PCSK9 transcription. However, the activation of PCSK9 promoter in the absence of a functional SRE suggest that compound **1** is an HNF1-α activator, effect that is counteracted by the inhibition of SREBP or others transcription factors involved in the transcription of PCSK9, such as STAT3 [43,44]. This data indicated that compound **1** acts at the transcriptional level, indeed the exogenous overexpression of PCSK9 FLAG tag with retroviral transduction was not affected by the incubation with compound **1** (Fig. 2J). This overexpression is, indeed, not mediated by the endogenous transcription factors but with the cytomegalovirus promoter.

We decided also to evaluate the *in vitro* effect of compound **1** co-incubated with simvastatin, to better explore its pharmacological profile, and the possible additive effect on the upregulation of the LDLR. The concentration of simvastatin was determined from our previous analysis [45]. As expected, simvastatin application to HepG2 cells, strongly induced PCSK9's expression after 24 h of incubation (Fig. 2C) through SREBP2 pathway activation [46]. On the contrary, we observed only a minimal effect on the LDLR expression (Fig. 3A and C), that possibly requires a longer incubation period (48 h–72 h). Interestingly, compound **1** significantly counteracted the effect of simvastatin on PCSK9 expression by reducing its levels by more than 65 % (Fig. 3A and B). At 12.5 μM concentration, compound **1** completely abrogated the induction of PCSK9 by simvastatin (Fig. 3A and B). Together with the inhibition on PCSK9 expression, we observed a significant induction of the LDLR after the incubation with lowest concentration of compound **1** (6.25 μM) in combination with simvastatin compared to the compound **1** alone (Fig. 3A and C).

These data suggest that this 2-pyridone derivative acts as inhibitor of the SREBP2 pathway activated by simvastatin and that, at lower concentration, the inhibitory effect on PCSK9 may improve the effect of simvastatin on the upregulation of the LDLR.

Pleased by the positive results observed with compound **1**, we extended our analysis on three structurally related analogues, already available in house: compounds **2**, **3**, and **4** (Fig. 4). The possible cytotoxicity of these compounds was determined by SRB assay under the same experimental conditions used for the hit compound **1**. On one hand, compound **2** showed to be cytotoxic at 50 and 100 μM, and with important despite not significant effect on cell viability at 25 μM concentration (Fig. 4A). On the other hand, compound **3** significantly affected HepG2 viability only at 100 μM, and compound **4** did not show any toxicity across all concentrations (Fig. 4B and C). The analysis on PCSK9 mRNA levels revealed that compound **2** was the less potent of this set of compounds, showing a significant effect only at 25 μM concentration, while compounds **3** and **4** showed very effective, and potent

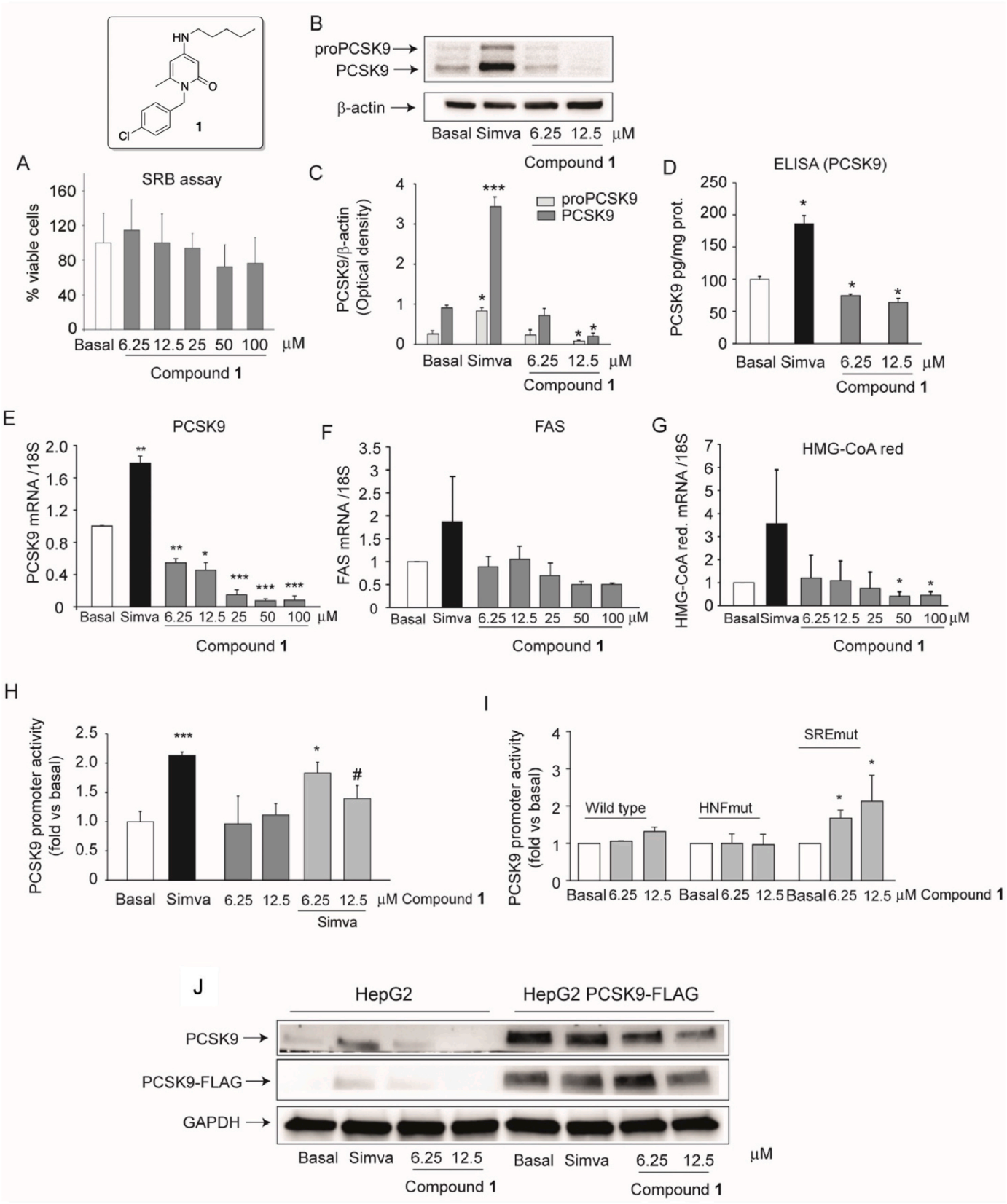

(caption on next page)

Fig. 2. Effect of compound 1 on cell viability and PCSK9 expression in HepG2. The cytotoxic effect was determined by SRB assay after 24 h incubation of HepG2 with 6.25, 12.5, 25, 50 or 100 μM of compound **1** (grey bar) or vehicle (basal, white bar) (A). Expression of proPCSK9 (light grey bar) and PCSK9 (dark grey bar) was evaluated by Western blot analysis. The densitometric readings were evaluated using the ImageLab™ software and the optical density was normalized over β-actin signal, used as a loading control (B and C). PCSK9 secretion from conditioned media was measured by ELISA assay under different experimental conditions: basal, after treatment with simvastatin 5 μM, and 6.25 or 12.5 μM of compound **1** (D). PCSK9, FAS and HMG-CoA reductase mRNA expression, with 18S as endogenous control, were measured by Quantitative real-time PCR (E, F, and G). PCSK9 promoter activity was determined under basal condition and after treatment with simvastatin 5 μM, and 6.25 or 12.5 μM of compound **1** (H). The same analysis was performed with PCSK9 promoter carrying HNF and SRE mutations (I). Exogenously expression of PCSK9-FLAG tag was detected from HepG2 overexpressing PCSK9 with anti-FLAG and anti-PCSK9 antibody (J). Data are shown as mean ± SD of three independent experiments and analyzed by means of one-way ANOVA. *$p < 0.05$; **$p < 0.01$; ***$p < 0.001$ vs Basal. #$p < 0.05$ vs simvastatin. Abbreviations: Simva: simvastatin (40 μM); SRB: sulforhodamine B; FAS: fatty-acid synthase; HMG-CoA: hydroxy-methyl-glutaryl-CoA reductase.

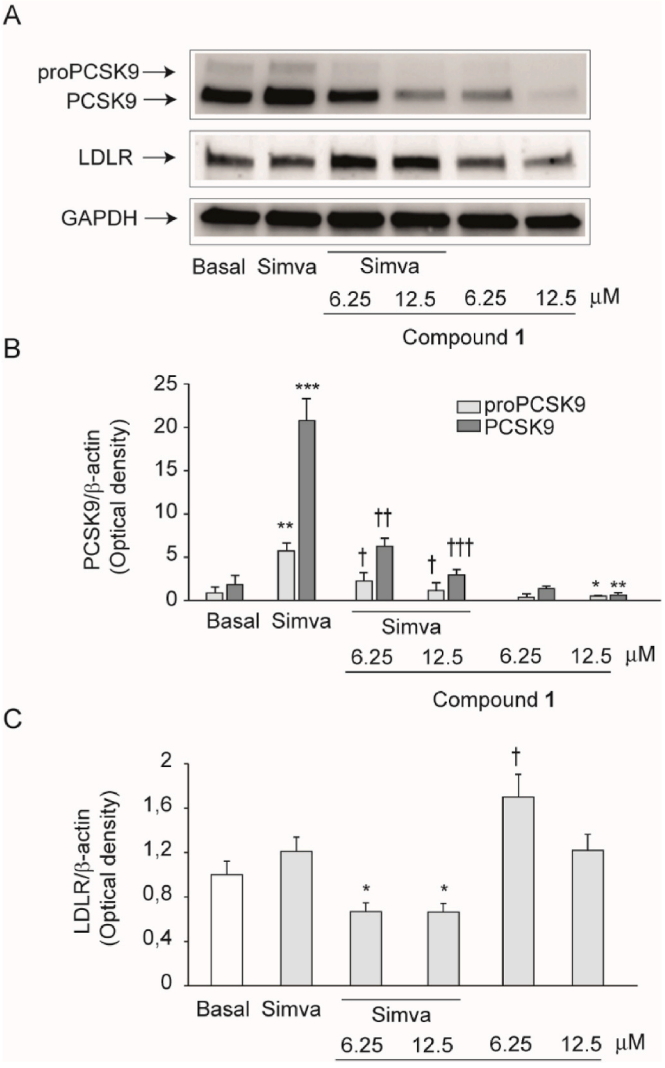

Fig. 3. Effect of combination of compound 1 and simvastatin on PCSK9 and LDLR expression in HepG2 cells. proPCSK9 (light grey, B), PCSK9 (dark grey, B) and LDLR (grey, C) protein levels were evaluated by Western blot analysis and normalized to β-actin, used as a loading control. Densitometric readings were evaluated using the ImageLab™ software. Data are shown as mean ± SD of three independent experiments and analyzed by means of one-way ANOVA test *$p < 0.05$; **$p < 0.01$; ***$p < 0.001$ vs Basal. #$p < 0.05$; ##$p < 0.01$; ###$p < 0.001$ vs Simva. Abbreviations: Simva: simvastatin (40 μM); LDLR: low-density lipoprotein receptor.

inhibition of PCSK9 expression (Fig. 4D). Therefore, we investigated the effect of **3** and **4** on protein expression by Western blot analysis, getting results consistent with those of mRNA expression (Fig. 4E and F)

Once verified the *in vitro* anti-PCSK9 effect of additional 2-pyridone derivatives, we started a hit expansion campaign to define the preliminary structure-activity-relationships (SAR) of this class of compounds, by synthesis and biological evaluation of a focused collection of new derivatives. Adopting the synthetic procedures A-C shown in Scheme 1, we prepared a collection of functionalized symmetric derivatives (**5a-f**), asymmetric derivatives (**7a-l**), and N-acylated derivatives (type **8a,b**) illustrated in Table 1. The commercial 4-hydroxy-6-methyl-2-pyrone, also known as triacetic acid lactone (TAL), and a series of functionalized amines were combined under different reaction conditions to achieve all the desired derivatives. Compounds **5a-f**, deriving from a nucleophilic attack on the TAL substrate by 2 equivalents of the opportune amine (R_1NH_2), were prepared adopting a solvent-free one-step microwave-assisted procedure (Scheme 1). The asymmetric derivatives **7a-l** required instead a 2-steps procedure (Scheme 1, procedure B). First, the intermediates **6a-f** were synthesized upon nucleophilic attack of the opportune amine (R_1NH_2, 1 equivalent) on TAL, using water as solvent to limit the formation of the symmetric derivatives **5**. In the second step, the isolated intermediates **6a-f** were further functionalized by reaction with different amines (R_2NH_2) under microwave heating at 160 °C in DME as solvent, thus affording the desired compounds **7a-l**. Finally, we further expanded the decoration of the 2-pyridone chemotype by functionalizing the NH group of two representative members of the symmetric and asymmetric derivatives: compounds **5c** and **7g** were thus reacted with acetyl chloride in DCM under microwaves heating, affording compounds **8a,b**. By exploiting these three simple, fast and (sometimes) green procedures, it was possible to synthesize the collection of derivatives reported in Table 1, which is characterized by a series of lipophilic substituents (R_1 and R_2) similar to those present in the hit compound **1**. The methoxybenzyl substituents of compounds **5e**, **5f**, and **7l**, were chosen for the structural similarity with berberine, since the 2-pyridones might also have a similar mechanism of action.

In order to identify improved analogues of the hit compound **1**, the newly synthesized molecules were initially tested at fixed concentration of 5 μM for their cytotoxicity on HepG2 cells and for their effect on PCSK9 and LDLR by Western blot analysis after overnight incubation. This concentration was selected starting from the observation that compound **1** was active from 6.25 μM. Under these conditions, all compounds showed no impact on cell viability (>95 %, data not shown) and, compared to untreated cells, a significant reduction of both proPCSK9 and mature PCSK9 was observed for compounds **5c** and **7i** (Fig. 5). More importantly, **5c**, but not **7i**, determined a significant induction of the LDLR. The inhibitory activity of compound **5c** on PCSK9 expression was most potent and effective than **1**, **2**, **3**, and **4**, by almost completely abrogating the expression of the target at 5 μM concentration (compare Fig. 3A, 4E and 5A), and showing significant activity at 2.5 μM (Fig. 6B and D). Intriguingly, also compound **5d** highly increased the expression of LDLR, by almost 3 folds; however, this effect was associated with no changes on proPCSK9 expression and a partial increase of PCSK9 (Fig. 5). From these analysis, compound **5c** seemed the most promising and was further tested for its capability to inhibit PCSK9 expression and to induce the LDLR in combination with simvastatin (Fig. 6). The determination of PCSK9 into conditioned media by ELISA assay further confirmed the strong inhibitory effect of compound **5c** on PCSK9 expression, with a complete block of its secretion from HepG2 cells at both 5 and 10 μM concentrations (Fig. 6A). Interestingly, compound **5c** counteracted the induction of PCSK9 by simvastatin, and was

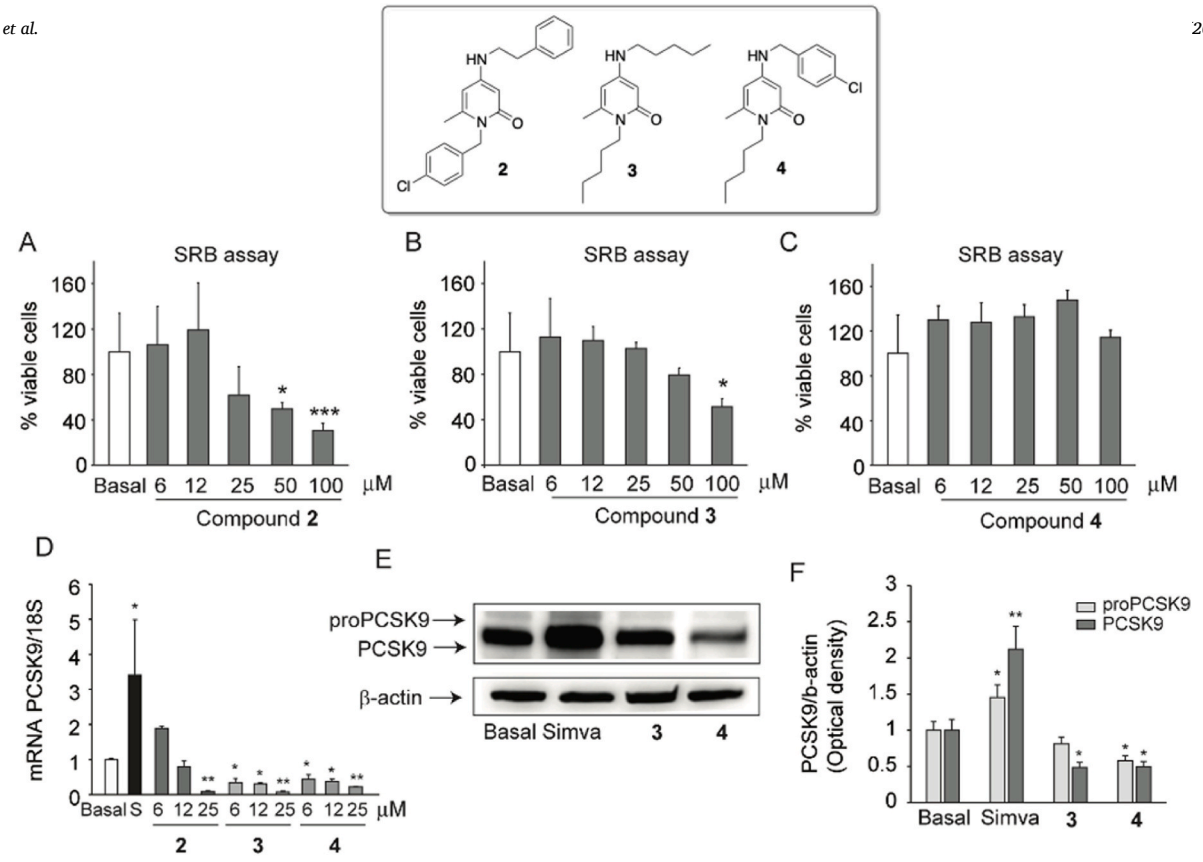

Fig. 4. Effect of compounds 2, 3 and 4 on cell viability and PCSK9 expression in HepG2 cells. The cytotoxic effect was determined by SRB assay after 24 h incubation of HepG2 with indicated concentrations of **2**, **3**, and **4** (A, B, and C). mRNA expression of PCSK9 was determined by Quantitative real-time PCR (D). PCSK9 expression was evaluated by Western blot analysis at 5 µM concentration (E). β-actin was used as a loading control and densitometric readings were evaluated using the ImageLab™ software, and the relative intensity of the bands are shown in the histograms (F). The data are expressed as mean ± SD of three independent experiments. *p < 0.05; **p < 0.01; vs Basal by one-way ANOVA. Simva: simvastatin (40 µM).

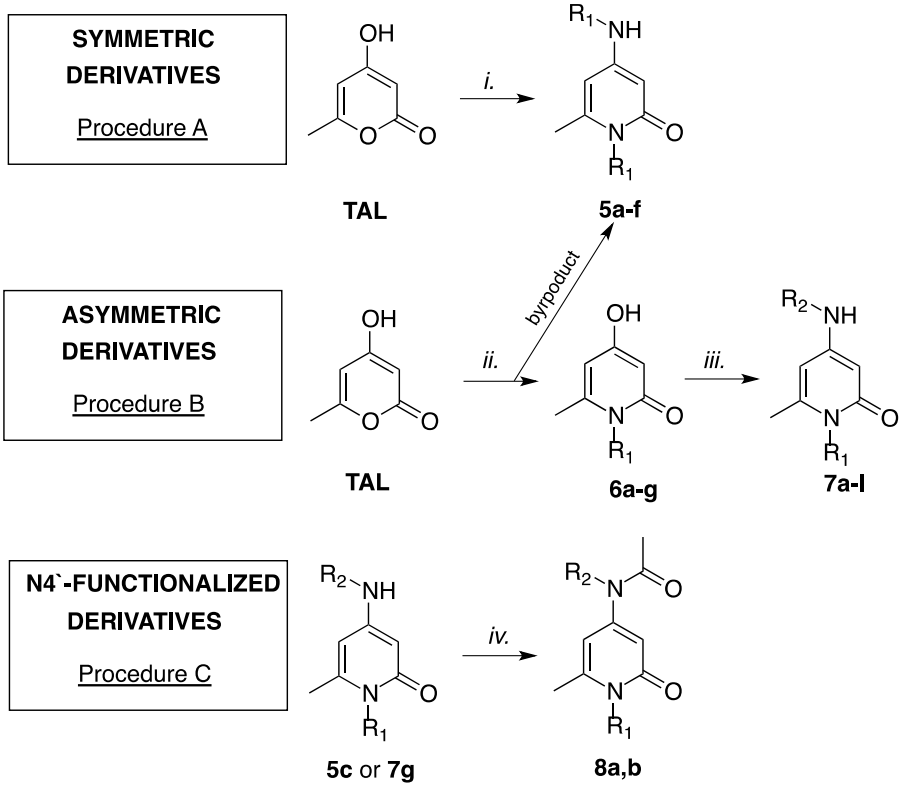

Scheme 1. Reagents and conditions: Procedure A: *i.* R_1NH_2 (2 eq.), neat, 120 °C µW, 6–9 min. Procedure B: *ii.* R_1NH_2 (1 eq.), H_2O, reflux, 2–4 h; *iii.* R_2NH_2 (1 eq.), DME, 160 °C µW, 10 min. Procedure C: *iv.* acetyl chloride (1.5 eq), pyridine (1.0 eq), DCM, 45 °C µW, 15 min.

associated with an additive effect on the expression of the LDLR by statin (Fig. 6B–D). Indeed, while compound **5c** alone had a moderate effect, it increased the simvastatin-induced LDLR expression and, consequently, the relative ratio LDLR/PCSK9 (Fig. 6E). Thus, these data suggest that compound **5c** may probably have a minor effect on cholesterol levels, since its action on the LDLR is limited. Instead, this molecule may be considered a booster of the hypocholesterolemic activity of statins, by inhibiting the PCSK9 expression. It is still unclear how the compound inhibited the PCSK9 without affecting the LDLR expression, however, it is tempting to speculate that **5c** interfere specifically with the transcription of PCSK9, a gene dependent not solely from SREBP, as the LDLR, but also by HNF-1α [47].

Finally, compound **5c** was administered to wild type C57BL/6J mice to preliminarily evaluate its *in vivo* tolerability in comparison with SBC-115076, a commercially available PCSK9 modulator [14]. The latter compound is known to act by inhibiting the PCSK9-LDLR interaction and was tested in C57BL/6 mice at 4 mg/kg dosage [48]. To evaluate the *in vivo* safety of compound **5c**, it was subcutaneously administered (SQ-inj) at 40 mg/kg, ten time the dosage of SBC-115076, for seven consecutive days. Body weight maintenance was daily recorded throughout the entire experimental period and the weight variation (%) with respect of basal measure (average of days −3 to −1) was measured. Our results demonstrated that **5c** administration did not induce any significant effect in analyzed parameters (Fig. 7A). In addition, a modified SHIRPA test was used to monitor general health status such as phenotype, sensory, and neuropsychiatric functions. Specifically, the spontaneous locomotor activity was measured before and after daily repeated treatment in order to assess any changes due to treatment. Results did not indicate significant differences in the average distance travelled during test session (Fig. 7B); in fact, the index of environmental exploration gradually reduced as a function of time and repeated sessions, independently by **5c** treatment. Moreover, no differences were detected on other parameters as well as the mean speed and % time exploring corners and arena, as index of anxiety (results not being significant are not shown).

As concerns other phenotypical observations measured by SHIRPA protocol, all experimental mice, regardless treatment group, were active and responsive to operator stimulations, without any sign of suffering, such as defect in urination and defecation, tremor or changes in fur sheen and abnormal secretions (data not shown). Furthermore, a macroscopic analysis of dissected organs (brain, spleen, liver, kidney and gut) was performed after mice sacrifice and did not evidence abnormalities between **5c**-treated groups with respect to vehicle. Histopathological assessment of liver sections did not reveal abnormal arrangement of hepatocytes, inflammatory cells infiltration or cellular necrosis, indicating that compound **5c** did not cause hepatic toxicity in comparison with vehicle-treated mice (Fig. 7C and D). In line with this observation, SBC-115076 and compound **5c** showed a reduction of ALT plasma levels (Fig. 7H). Albeit the experiment was designed to assess the *in vivo* tolerability of compound **5c**, PSCK9 was quantified both in liver (fold change of mRNA; Fig. 7E) and plasma (pg/ml PCSK9 protein; Fig. 7G), together with plasma total cholesterol level (mg/dl; Fig. 7F). Despite the absence of statistically significant differences, a slight increase of PCSK9 was detected in mice treated with SBC-115076, which is in line with previous experiments conducted on the same compound [35] and on other compound with a similar mechanism of action [49], while a slight decrease of PCSK9 was observed in mice treated with **5c**. No change in plasma total cholesterol level were detected, but this could be very likely due to an insufficient length of treatment or dosage [36], poor biodistribution and could be better detected on mice fed with high fat diet.

Overall, these data suggest that the subcutaneous injection of 40 mg/kg of compound **5c** for 7 days did not induce any sign of toxicity and was well tolerated by treated mice; proof of *in vivo* efficacy should be obtained in the future with this promising anti-PCSK9 compound through a series of dedicated experiments.

3. Conclusion

In the present study we identified a new class of anti-PCSK9 small-molecules potentially able to overcome the drawbacks of anti-PCSK9 biological drugs. Although a certain number of small molecules with anti-PCSK9 inhibitory activity has been reported in the literature, PCSK9 is not easily druggable and an orally administrable small-molecule drug is still missing. To overcome these limitations, we have conducted a phenotypic drug discovery (PDD) campaign aimed at the identification of new small molecules inhibitors able to modulate the PCSK9 activity in a functional assay, independently from the specific binding pocket. This approach can better address the complexity of drug action than a simplistic model in which the therapeutic effects are determined by the occupancy of a specific pocket of a target protein and also provide an early toxicity estimation. By evaluating the intracellular PCSK9 expression of HepG2 cells treated with 50 different chemotypes from our internal collection, the hit compound **1** was identified as a promising PCSK9 inhibitor and expanded in a focused collection of derivatives. Among the newly synthesized molecules, compound **5c** was identified as the most potent and promising candidate: at 5 μM, it completely blocked the PCSK9 secretion from HepG2 cells, significantly increasing the LDLR expression. Importantly, **5c** acted synergistically with simvastatin, further increasing the LDLR expression and counteracting the statin-induced PCSK9 expression. Further analyses are required to fully elucidated its molecular mechanism of action, the selectivity towards other genes involved in lipid metabolism, and the capability of improving the LDL uptake from cell, alone or in combination with simvastatin.

Finally, a preliminarily evaluation of the *in vivo* tolerability of compound **5c** showed no sign of toxicity or behavior modifications. Thus, the results of our study pave the way for the generation of a new set of compounds interfering with PCSK9 expression that may be used as booster of statin treatment. Future studies will be dedicated to investigating the *in vivo* hypocholesterolemic effect in the absence or presence of simvastatin. From our data it is, however, possible to envision a problem of selectivity of our compounds towards PCSK9 compared to other genes involved in cholesterol metabolism. The selection of the appropriate dose for *in vivo* analysis may, indeed, required attention.

4. Experimental section

4.1. Chemistry

General. All commercially available chemicals were purchased from Fisher Scientifics and Fluorochem and, unless otherwise noted, used without any previous purification. Solvents used for work-up and purification procedures were of technical grade. TLC was carried out using Sigma-Aldrich TLC plates (silica gel on Al foils, SUPELCO Analytical, Merck 60 F254 silica plates). Where indicated, products were purified by silica gel flash chromatography on columns packed with Merck Geduran Si 60 (40–63 μm), or Merck 60 silica gel, 230–400 mesh. ^{1}H and ^{13}C NMR spectra were recorded on BRUKER AVANCE 400 MHz spectrometers. Chemical shifts (δ scale) are reported in parts per million relative to TMS. ^{1}H NMR spectra are reported in this order: multiplicity and number of protons; signals were characterized as: *s* (singlet), *d* (doublet), *dd* (doublet of doublets), *ddd* (doublet of doublet of doublets), *t* (triplet), *m* (multiplet), *bs* (broad signal). ESI-mass spectra were recorded on an API 150EX apparatus and are reported in the form of (*m*/*z*). Elemental analyses were performed on a PerkinElmer PE 2004 elemental analyzer, and the data for C, H, and N are within 0.4 % of the theoretical values. Melting points were taken using a Gallenkamp melting point apparatus and were uncorrected. IR spectra were recorded using "Agilent Technologies FTIR", sample scans: 24; background scans: 16; wavelength range: 4000-650 nm; Apodization: Happ-Genzel.

Microwave Irradiation Experiments. Microwave reactions were conducted using a CEM Discover Synthesis Unit (CEM Corp., Matthews,

Table 1
Library of 4-amino-2-pyridones, prepared as analogues of the hit compound **1**.

Entry	Compound	Procedure	R_1	R_2	R_3
1	**5a**	A	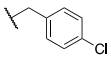	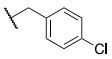	H
2	**5b**	A	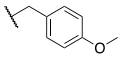	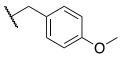	H
3	**5c**	A	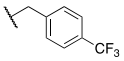	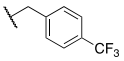	H
4	**5d**	B			H
5	**5e**	A	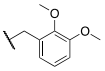	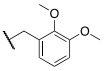	H
6	**5f**	A	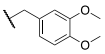	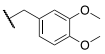	H
7	**7a**	B			H
8	**7b**	B			H
9	**7c**	B			H
10	**7d**	B			H
11	**7e**	B			H
12	**7f**	B		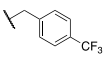	H
13	**7g**	B	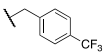		H
14	**7h**	B	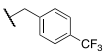		H
15	**7i**	B	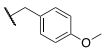		H
16	**7j**	B	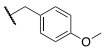		H
17	**7k**	B		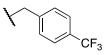	H
18	**7l**	B	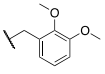		H
19	**8a**	C	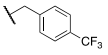		
20	**8b**	C	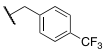		

NC). The machine consists of a continuous focused microwave power delivery system with an operator-selectable power output from 0 to 300 W. The temperature inside the reaction vessel was monitored using a calibrated infrared temperature control mounted under the reaction vessel. All experiments were performed using a stirring option whereby the reaction mixtures were stirred by means of a rotating magnetic plate located below the floor of the microwave cavity and a Teflon-coated magnetic stir bar in the vessel.

4.1.1. General procedure A

In a 10 mL microwave tube, equipped with magnetic stir bar and septum, a mixture 4-hydroxy-6-methyl-2-pyrone (100 mg, 1 equivalent, 0.79 mmol) and the opportune amine specified below (2–3 equivalents) was heated at 120 °C for 6 min in the microwave apparatus (maximum power input: 300 W; maximum pressure: 250 psi; power max: OFF; stirring: ON). After cooling to room temperature, the solid was filtered on Buchner, washed with Et_2O and then purified by flash chromatography.

4.1.1.1. 1-(4-chlorobenzyl)-4-((4-chlorobenzyl)amino)-6-methylpyridin-2(1H)-one (5a). Compound **5a** was prepared according to General procedure A, using as opportune amine the 4-chlorobenzylamine (2

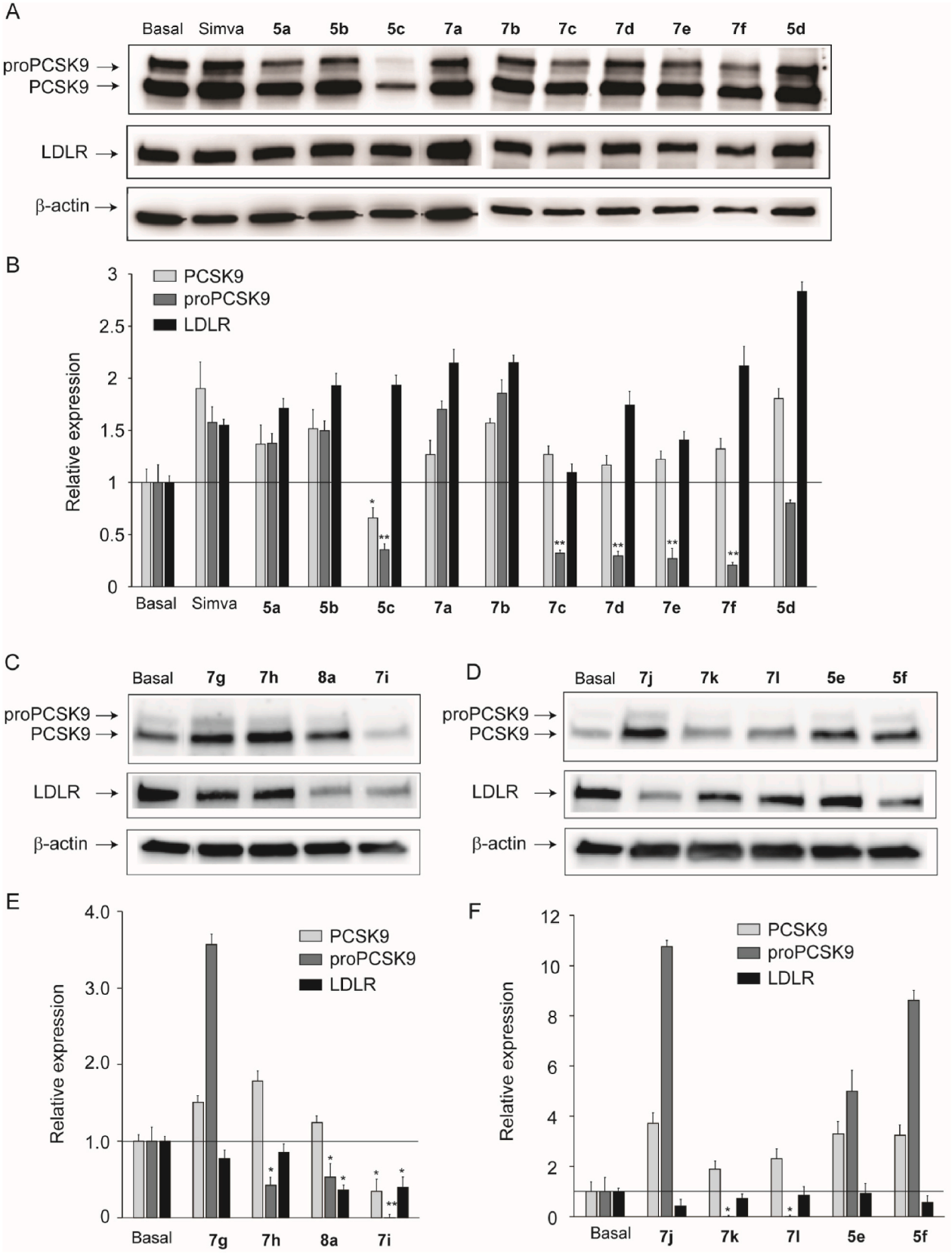

Fig. 5. Effect of 2-pyridone derivatives on PCSK9 and LDLR expression in HepG2 cells. PCSK9 and LDLR expression was evaluated by Western blot analysis (A and C). β-actin was used as a loading control and densitometric readings were evaluated using the ImageLab™ software, and the relative intensity of the bands are shown in the histograms (B, E and F). Simva: simvastatin (40 μM).

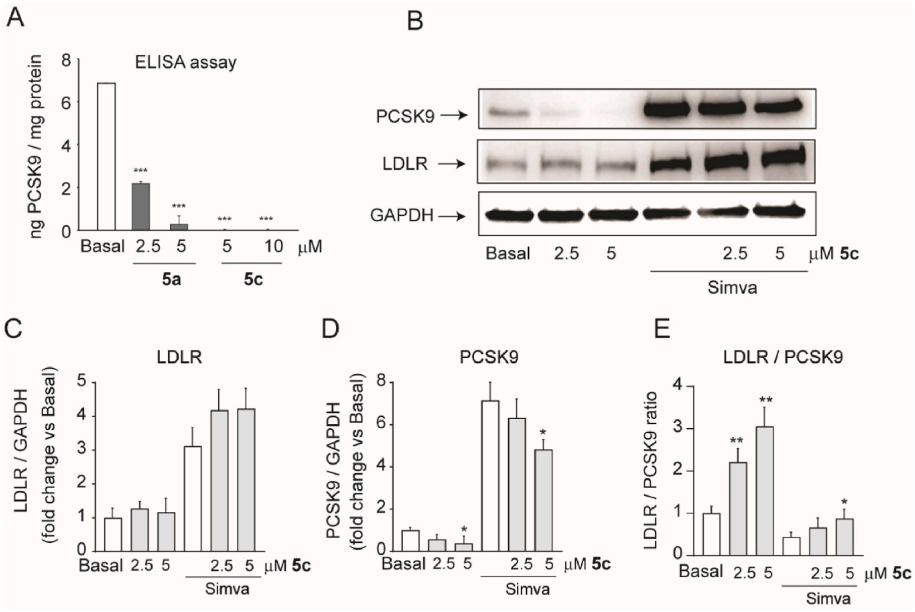

Fig. 6. Effect of combination of compound 5c and simvastatin on PCSK9 and LDLR expression in HepG2 cells. A) PCSK9 levels were determined by ELISA from conditioned media after treatment with indicated concentrations of compound **5a** and **5c**. The data were normalized with total protein content of HepG2 cells. B) PCSK9 and LDLR expression was evaluated by Western blot analysis after incubation of HepG2 cells with compound **5c** in the presence or absence of simvastatin (40 µM). GAPDH was used as a loading control and densitometric readings were evaluated using the ImageLab™ software, and the relative intensity of the bands are shown in the histograms (C, D and E). Simva: simvastatin.

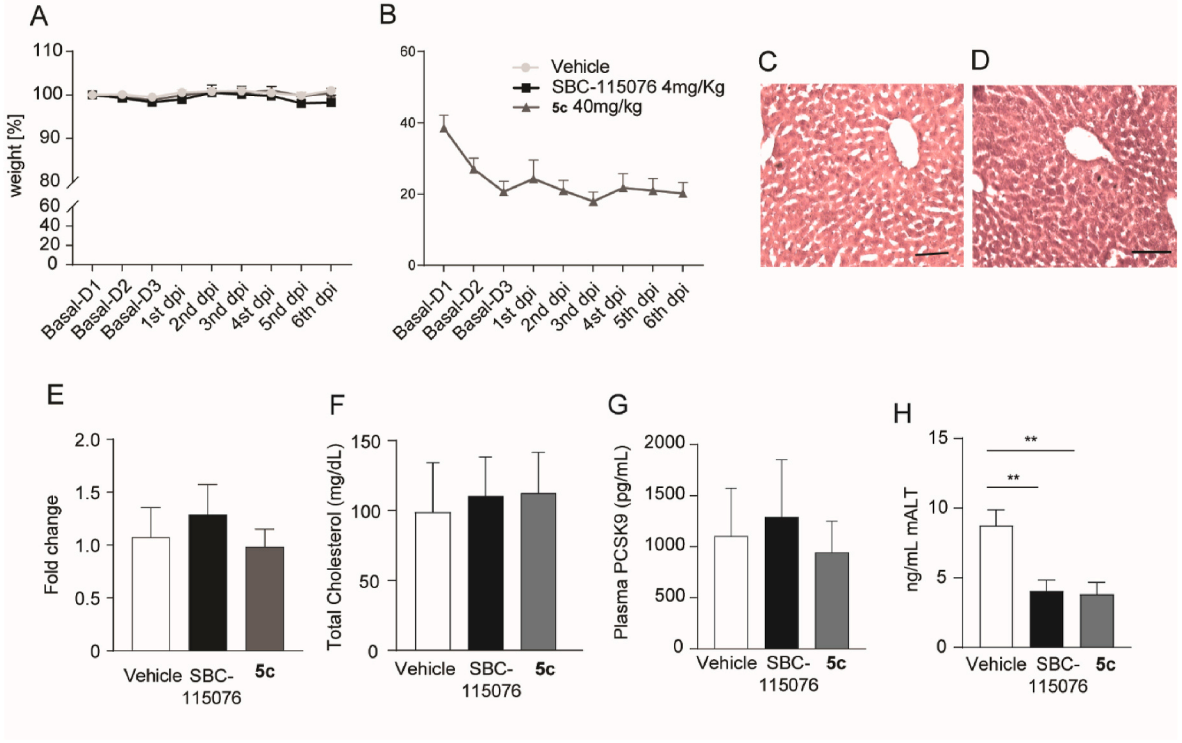

Fig. 7. Effects of subacute 5c treatment on behavioral and biochemical parameters *in vivo*. A-B) The analysis of body weight changes (A) and spontaneous locomotor activity (B) were similar in all experimental groups - vehicle (light grey), SBC-115076 (black) or **5c** compound (dark grey) - showing the absence of toxicity due to subacute injections of **5c** compound. **C-D)** Histological analysis of hepatic tissues from vehicle (C) or **5c**-treated mice (D). **E)** *Pcsk9* mRNA expression in the liver of mice treated with vehicle (white bar), SBC-115076 (black bar) or **5c** compound (dark grey). Data are presented as fold change normalized over vehicle group mean and calibrated over GAPDH housekeeping gene. **F-G)** Total cholesterol (F) and PCSK9 plasma levels (G) were determined by biochemical and ELISA assay, respectively. **H**) ALT plasma levels were determined by ELISA kit. Data are shown as mean ± SEM. Experimental groups: Vehicle, n = 5; SBC-115076, n = 6; **5c**, n = 6. Abbreviations: D1 = Day 1; dpi = day post injection.

equivalents, 193 μL, 1.58 mmol). The reaction was monitored by TLC analysis ($CHCl_3$/MeOH 96/4; Rf = 0.4). The crude of the reaction was purified by flash chromatography ($CHCl_3$/MeOH 99/1–98/2), affording the desired product in 50 % yield (149.30 mg, 0.40 mmol).

^{1}H NMR (300 MHz, DMSO-d_6) δ 7.37 (m, 6H), 7.11 (d, 2H), 7.09 (bs, 1H), 5.70 (d, 1H, J = 1.77 Hz), 5.13 (d, 1H, J = 2.19 Hz), 5.08 (s, 1H), 5.24 (d, 2H, J = 5.88 Hz), 2.08 (s, 3H). ^{13}C NMR (100.6 MHz, $CDCl_3$) δ 163.3, 154.9, 145.2, 138.0, 137.4, 131.3, 128.5, 98.9, 88.7, 44.6, 44.3, 19.9. MS (ESI) m/z 373.2 $[M+H]^+$

4.1.1.2. 1-(4-methoxybenzyl)-4-((4-methoxybenzyl)amino)-6-methylpyridin-2(1H)-one (5b). Compound **5b** was prepared according to General procedure A, using as opportune amine the 4-Methoxybenzylamine (2 equivalents, 206 μL, 1.58 mmol). The reaction was monitored by TLC analysis ($CHCl_3$/MeOH 96/4; Rf = 0.4). The crude of the reaction was purified by flash chromatography, ($CHCl_3$/MeOH 99/1–98/2), affording the desired product in 70 % yield (201.50 mg, 0.55 mmol).

^{1}H NMR (300 MHz, $CDCl_3$) δ 7.26 (2, 2H, J = 8.76 Hz), 7.13 (d, 2H, J = 8.49 Hz), 6.90 (d, 2H, J = 8.61 Hz), 6.84 (d, 2H J = 8.67 Hz), 5.64 (s, 1H), 5.49 (s, 1H), 5.19 (s, 2H), 4.22 (d, 2H, J = 4.65 Hz), 3.82 (s, 3H), 3.79 (s, 3H), 2.17 (s, 3H). ^{13}C NMR (100.6 MHz, $CDCl_3$) δ 162.8, 155.1, 144.5, 137.6, 137.0, 133.2, 127.6, 99.9, 88.8, 55.6, 44.6, 44.1, 20.0. MS (ESI) m/z 365.1 $[M+H]^+$.

4.1.1.3. 6-Methyl-1-(4-(trifluoromethyl)benzyl)-4-((4-(trifluoromethyl) benzyl)amino)pyridin-2(1H)-one (5c). Compound **5c** was prepared according to General procedure A, using as opportune amine the 4-(trifluoromethyl)benzylamine (2 equivalents, 225 μL, 1.58 mmol). The reaction was monitored by TLC analysis ($CHCl_3$/MeOH 96/4; Rf = 0.4). The crude of the reaction was purified by flash chromatography ($CHCl_3$/MeOH 99/1–98/2), affording the desired product in 55 % yield (180.40 mg, 0.43 mmol).

^{1}H NMR (400 MHz, $CDCl_3$) δ 7.505 (d, 2H, J = 7.83 Hz), 7.46 (d, 2H, J = 7.83 Hz), 7.33 (d, 2H, J = 7.83 Hz), 7.16 (d, 2H, J = 7.83 Hz), 5.53 (d, 1H, J = 1.89 Hz), 5.46 (d, 1H, J = 1.89 Hz), 5.18 (bs, 2H), 4.79 (bs, 1H), 4.26 (d, 2H, J = 4.60 Hz), 2.04 (s, 3H).^{13}C NMR (100.6 MHz, $CDCl_3$) δ 163.5, 153.9, 144.5, 140.7, 140.5, 128.8 (q, $J_{C\text{-}F}$ = 32.51 Hz), 128.5 (q, $J_{C\text{-}F}$ = 32.51 Hz), 126.4, 125.6, 124.7, 124.7, 123.0 (q, $J_{C\text{-}F}$ = 271.69 Hz), 99.0, 89.9, 45.3, 44.9, 19.4. MS (ESI) m/z 441.2 $[M+H]^+$, 463.3, $[M+Na]^+$.

4.1.1.4. 1-(2,3-dimethoxybenzyl)-4-((2,3-dimethoxybenzyl)amino)-6-methylpyridin-2(1H)-one (5e). Compound **5e** was prepared according to General procedure A, using as opportune amine the 2,3-dimethoxybenzylamine (3 equivalents, 326 μL, 2.37 mmol). The reaction was monitored by TLC analysis (DCM/MeOH 96/4; Rf = 0.4). The crude of the reaction was purified by flash chromatography (DCM/MeOH 99/1–97/3), affording the desired product in 21 % yield (70.60 mg, 0.17 mmol).

^{1}H NMR (300 MHz, $CDCl_3$) δ 6.94 (t, 1H, J = 2.29 Hz), 6.85 (t, 1H, J = 8.07 Hz), 6.80 (dt, 2H, J = 7.94, 1.20 Hz), 6.10 (d, 1H, J = 7.25 Hz), 6.40 (d, 1H, J = 7.76 Hz), 5.56 (d, 1H, J = 2.59 Hz), 5.45 (s, 1H), 5.21 (s, 2H), 4.60 (s, 1H), 4.22 (d, 2H, J = 7.14 Hz), 3.79–3.78 (m, 9H), 3.77 (s, 3H), 2.00 (s, 3H). ^{13}C NMR (100.6 MHz, $CDCl_3$) δ 163.9, 153.9, 151.7, 151.3, 146.0, 144.9, 144.7, 130.4, 130.3, 123.4, 123.2, 119.9, 117.4, 111.0, 110.0, 98.8, 89.6, 59.8, 59.6, 54.8, 54.7, 41.2, 39.9, 19.2. MS (ESI) m/z 425.2 $[M+H]^+$.

4.1.1.5. 1-(3,4-dimethoxybenzyl)-4-((3,4-dimethoxybenzyl)amino)-6-methylpyridin-2(1H)-one (5f). Compound **5f** was prepared according to General procedure A, using as opportune amine the 3,4-dimethoxybenzylamine (3 equivalents, 364 μL, 2.37 mmol). The reaction was monitored by TLC analysis (DCM/MeOH 96/4; Rf = 0.4). The crude of the reaction was purified by flash chromatography (DCM/MeOH 99/1–97/3), affording the desired product in 40 % yield (134.14 mg, 0.32 mmol).

^{1}H NMR (300 MHz, $CDCl_3$) δ 6.78–6.65 (m, 6H), 5.51 (d, 1H, J = 2.29 Hz), 5.45 (s, 1H), 5.06 (s, 2H), 4.56 (s, 1H), 4.10 (d, 2H, J = 5.74 Hz), 3.77 (s, 6H), 3.73 (s, 3H), 3.72 (s, 3H), 2.07 (s, 3H). ^{13}C NMR (100.6 MHz, $CDCl_3$) δ 163.8, 153.8, 148.2, 148.2, 147.5, 147.1, 144.7, 129.2, 129.1, 118.9, 117.6, 110.3, 110.1, 109.9, 109.1, 98.7, 89.7, 54.9, 54.9, 45.8, 44.9, 42.3, 41.7, 19.5. MS (ESI) m/z 425.2 $[M+H]^+$.

4.1.2. General procedure B. Step 1 (intermediate synthesis)

To a solution of 4-hydroxy-6-methyl-2-pyrone (500 mg, 3.96 mmol, 1 equivalent) in H_2O (10 mL), the proper amine (3.96 mmol, 1 equivalent) was added. The resulting mixture was refluxed until complete conversion of the starting materials (3–24 h), monitored by TLC. The solid mass was filtrated under vacuum, washed with diethyl ether and purified by silica gel flash chromatography to give the desired compounds as white solids.

4.1.2.1. 4-Hydroxy-1-isopentyl-6-methylpyridin-2(1H)-one (6a). Compound **6a** was prepared according to General procedure B, using as opportune amine the Isopentylamine (459.6 μL, 3.96 mmol). The reaction mixture was refluxed for 12 h, and upon completion of the reaction (monitored by TLC analysis: DCM/MeOH 93/7; Rf = 0.4). The resulting solid was filtrated under vacuum, washed with diethyl ether and purified by flash chromatography (DCM/MeOH 99/1–95/5), affording the desired product in 83 % yield (641.80 mg, 3.29 mmol).

^{1}H NMR (300 MHz, DMSO-d_6) δ 10.32 (s, 1H), 5.73 (s, 1H), 5.47 (s, 1H), 3.86–3.80 (m, 2H), 2.29 (s, 3H), 1.65–1.56 (m, 1H), 1.41–1.34 (m, 2H), 0.91 (d, J = 6.6 Hz, 6H). MS (ESI) m/z 196.2 $[M+H]^+$, 218.3 $[M+Na]^+$.

4.1.2.2. 1-Benzyl-4-hydroxy-6-methylpyridin-2(1H)-one (6b). Compound **6b** was prepared according to General procedure B, using as opportune amine the Benzylamine (432.6 μL, 3.96 mmol). The reaction mixture was refluxed for 12 h, and upon completion of the reaction (monitored by TLC analysis: DCM/MeOH 93/7; Rf = 0.4). The resulting solid was filtrated under vacuum, washed with diethyl ether and purified by flash chromatography (DCM/MeOH 99/1–95/5), affording the desired product in 89 % yield (758.60 mg, 3.52 mmol).

^{1}H NMR (300 MHz, DMSO-d_6) δ 10.31 (s, 1H), 7.36–7.26 (m, 5H), 5.54 (s, 1H), 5.47 (s, 1H), 4.25 (d, J = 5.3 Hz, 2H), 2.27 (s, 3H). MS (ESI) m/z 216.2 $[M+H]^+$, 238.3 $[M+Na]^+$.

4.1.2.3. 4-Hydroxy-6-methyl-1-pentylpyridin-2(1H)-one (6c). Compound **6c** was prepared according to General procedure B, using as opportune amine the Pentylamine (459.6 μL, 3.96 mmol). The reaction mixture was refluxed for 12 h, and upon completion of the reaction (monitored by TLC analysis: DCM/MeOH 93/7; Rf = 0.4). The resulting solid was filtrated under vacuum, washed with diethyl ether and purified by flash chromatography (DCM/MeOH 99/1–95/5), affording the desired product in 79 % yield (610.90 mg, 3.13 mmol).

^{1}H NMR (300 MHz, DMSO-d_6) δ 10.32 (s, 1H), 5.98 (s, 1H), 5.91 (s, 1H), 3.96–3.91 (m, 2H), 2.34 (s, 3H), 1.67–1.62 (m, 2H), 1.37–1.32 (m, 4H), 0.93–0.89 (m, 3H). MS (ESI) m/z 196.4 $[M+H]^+$, 218.4 $[M+Na]^+$.

4.1.2.4. 4-Hydroxy-1-isobutyl-6-methylpyridin-2(1H)-one (6d). Compound **6d** was prepared according to General procedure B, using as opportune amine the Isobutylamine (394.0 μL, 3.96 mmol). The reaction mixture was refluxed for 12 h, and upon completion of the reaction (monitored by TLC analysis: DCM/MeOH 93/7; Rf = 0.4). The resulting solid was filtrated under vacuum, washed with diethyl ether and purified by flash chromatography (DCM/MeOH 99/1–95/5), affording the desired product in 90 % yield (645.90 mg, 3.56 mmol).

^{1}H NMR (300 MHz, DMSO-d_6) δ 10.30 (s, 1H), 6.05 (s, 1H), 5.95 (s, 1H), 3.83–3.82 (m, 2H), 2.34 (s, 3H), 2.21–2.14 (m, 1H), 0.94 (d, J = 6.5 Hz, 6H). MS (ESI) m/z 182.2 $[M+H]^+$, 204.3 $[M+Na]^+$.

4.1.2.5. 4-Hydroxy-6-methyl-1-(4-(trifluoromethyl)benzyl)pyridin-2(1H)-one (6e). Compound **6e** was prepared according to General procedure B, using as opportune amine the 4-(trifluoromethyl)benzylamine (564.3 μL, 3.96 mmol). The reaction mixture was refluxed for 3.5 h, and upon completion of the reaction (monitored by TLC analysis: DCM/MeOH 93/7; Rf = 0.4) The resulting solid was filtrated under vacuum, washed with diethyl ether and purified by flash chromatography (DCM/MeOH 99/1), affording the desired product in 40 % yield (449.00 mg, 1.58 mmol).

^{1}H NMR (300 MHz, DMSO-d_6) δ 10.59 (bs, 1H), 7.69 (d, 2H, J = 8.97 Hz), 7.30 (d, 2H, J = 7.98 Hz), 5.84 (dd, 1H, J = 2.64, 0.81 Hz), 5.62 (d, 1H, J = 2.61 Hz), 5.27 (bs, 2H), 2.16 (s, 3H). MS (ESI) *m/z* 284.1 $[M+H]^+$

4.1.2.6. 4-Hydroxy-1-(4-methoxybenzyl)-6-methylpyridin-2(1H)-one (6f). Compound **6f** was prepared according to General procedure B, using as opportune amine the 4-(trifluoromethoxy)benzylamine (604.6 μL, 3.96 mmol). The reaction mixture was refluxed for 3.5 h, and upon completion of the reaction (monitored by TLC analysis: DCM/MeOH 93/7; Rf = 0.4). The resulting solid was filtrated under vacuum, washed with diethyl ether and purified by flash chromatography (DCM/MeOH 99/1), affording the desired product in 34 % yield (449.00 mg, 1.58 mmol).

^{1}H NMR (300 MHz, DMSO-d_6) δ 10.48 (bs, 1H), 7.94 (d, 2H, J = 8.82 Hz), 6.88 (d, 2H, J = 8.76 Hz), 5.77 (dd, 1H, J = 2.62, 0.76 Hz), 5.58 (d, 1H, J = 2.61 Hz), 5.10 (bs, 2H), 3.71 (s, 3H), 2.17 (s, 3H). MS (ESI) *m/z* 246.1 $[M+H]^+$.

4.1.2.7. 1-(2,3-dimethoxybenzyl)-4-hydroxy-6-methylpyridin-2(1H)-one (6g). Compound **6g** was prepared according to General procedure B, using as opportune amine the 2,3-(dimethoxy)benzylamine (543.3 μL, 3.96 mmol). The reaction mixture was refluxed for 24 h, and upon completion of the reaction (monitored by TLC analysis: DCM/MeOH 93/7; Rf = 0.4). The resulting solid was filtrated under vacuum, washed with diethyl ether and purified by flash chromatography (DCM/MeOH 97/3–96/4), affording the desired product in 22 % yield (246.40 mg, 0.89 mmol).

^{1}H NMR (300 MHz, DMSO-d_6) δ 10.50 (s, 1H), 6.97–6.96 (m, 2H), 6.15 (dd, 1H, J = 5.1, 1.8 Hz), 5.82 (dd, 1H, J = 2.1, 0.6 Hz), 5.57 (d, 1H, J = 2.1 Hz), 5.15 (s, 2H), 3.81 (s, 3H), 3.79 (s, 3H), 2.14 (s, 3H). MS (ESI) *m/z* 276.1 $[M+H]^+$.

4.1.2.8. 1-Isopentyl-4-(isopentylamino)-6-methylpyridin-2(1H)-one (5d). Compound **5d** was obtained in amount sufficient for biological testing as byproduct of the reaction performed for synthesizing intermediate **6a**. According to General procedure B, using as opportune amine the Isopentylamine (459.6 μL, 3.96 mmol), the reaction mixture was refluxed for 12 h, and upon completion of the reaction (monitored by TLC analysis: DCM/MeOH 93/7; Rf = 0.4 for the intermediate **6a**, Rf = 0.6 for compound **5d**). The resulting solid was filtrated under vacuum, washed with diethyl ether and purified by flash chromatography (DCM/MeOH 99/1–95/5), affording the product in33 % yield (345.5 mg, 1.31 mmol).

^{1}H NMR (400 MHz, $CDCl_3$) δ 5.45 (s, 1H), 5.44 (s, 1H), 3.98 (s, 1H), 3.94–3.90 (m, 2H), 3.09–3.05 (m, 2H), 2.27 (s, 3H), 1.74–1.64 (m, 2H), 1.55–1.45 (m, 4H), 0.97 (d, J = 6.6 Hz, 6H), 0.94 (d, J = 6.6 Hz, 6H).^{13}C NMR (100.6 MHz, $CDCl_3$) δ 164.6, 154.6, 144.6, 99.4, 90.7, 42.1, 40.9, 37.9, 37.8, 26.5, 25.9, 22.5 (2C), 22.4 (2C), 20.2. MS (ESI) *m/z* 265.2 $[M+H]^+$.

4.1.3. General procedure B. Step 2

In a 10 mL microwave tube, equipped with magnetic stir bar and septum, a mixture of intermediate 6a–g and the opportune amine in dimethoxyethane (1 mL) was heated at 120 °C for 40 min in the microwave apparatus (maximum power input: 300 W; maximum pressure: 250 psi; power max: OFF; stirring: ON). After cooling to room temperature, the solvent was evaporated under reduced pressure and the residue was purified by silica gel flash chromatography, affording the desired compounds as white solids.

4.1.3.1. 4-(Benzylamino)-1-isopentyl-6-methylpyridin-2(1H)-one (7a). Compound **7a** was prepared according to General procedure B, using as reactants intermediate **6a** (100 mg, 0.51 mmol) and benzylamine (1.5 equivalents, 84.1 μL, 0.77 mmol). The reaction was monitored by TLC analysis (DCM/MeOH 96/4; Rf = 0.4). The crude of the reaction was purified by flash chromatography (DCM/MeOH 99/1–98/2), affording the desired product in 28 % yield (39.80 mg, 0.14 mmol).

^{1}H NMR (400 MHz, $CDCl_3$) δ 7.35–7.26 (m, 5H), 5.52 (s, 1H), 5.49 (s, 1H), 4.61 (s, 1H), 4.24 (d, J = 5.4 Hz, 2H), 3.92–3.88 (m, 2H), 2.26 (s, 3H), 1.73–1.64 (m, 1H), 1.54–1.48 (m, 2H), 0.97 (d, J = 6.6 Hz, 6H).^{13}C NMR (100.6 MHz, $CDCl_3$) δ 164.5, 154.6, 144.8, 137.9, 128.7 (2C), 128.5, 127.5 (2C), 99.4, 91.3, 46.9, 42.1, 37.8, 26.5, 22.5 (2C), 20.3. MS (ESI) *m/z* 285.3 $[M+H]^+$, 307.3 $[M+Na]^+$.

4.1.3.2. 4-((4-Chlorobenzyl)amino)-1-isopentyl-6-methylpyridin-2(1H)-one (7b). Compound **7b** was prepared according to General procedure B, using as reactants intermediate **6a** (100 mg, 0.51 mmol) and 4-chlorobenzylamine (1.5 equivalents, 93.7 μL, 0.77 mmol). The reaction was monitored by TLC analysis (DCM/MeOH 96/4; Rf = 0.4). The crude of the reaction was purified by flash chromatography (DCM/MeOH 99/1–98/2), affording the desired product in 33 % yield (53.70 mg, 0.17 mmol).

^{1}H NMR (400 MHz, $CDCl_3$) δ 7.32–7.22 (m, 4H), 5.52 (s, 1H), 5.48 (s, 1H), 4.55 (s, 1H), 4.24 (d, J = 5.4 Hz, 2H), 3.93–3.89 (m, 2H), 2.28 (s, 3H), 1.73–1.67 (m, 1H), 1.55–1.49 (m, 2H), 0.97 (d, J = 6.6 Hz, 6H). ^{13}C NMR (100.6 MHz, $CDCl_3$) δ 164.4, 154.3, 144.9, 136.4, 133.3, 128.9 (2C), 128.7 (2C), 99.3, 91.5, 46.2, 42.2, 37.8, 26.5, 22.5 (2C), 20.3. MS (ESI) *m/z* 319.3 $[M+H]^+$, 341.3 $[M+Na]^+$.

4.1.3.3. 1-Benzyl-4-(isopentylamino)-6-methylpyridin-2(1H)-one (7c). Compound **7c** was prepared according to General procedure B, using as reactants intermediate **6b** (110 mg, 0.51 mmol) and Isopentylamine (1.5 equivalents, 89.3 μL, 0.77 mmol). The crude of the reaction was purified by flash chromatography (DCM/MeOH 99/1–98/2), affording the desired product in 36 % yield (52.20 mg, 0.18 mmol).

^{1}H NMR (400 MHz, $CDCl_3$) δ 7.22-7-13 (m, 3H), 7.07 (d, 2H J = 8.01 Hz), 5.50 (s, 1H), 5.43 (s, 1H), 5.17 (s, 2H), 4.15 (s, 1H), 3.03–3.01 (m, 2H), 2.05 (s, 3H), 1.59 (sep, 1H, J = 6.61 Hz), 1.41 (q, 2H, J = 7.87 Hz), 0.86 (s, 3H), 0.85 (s, 3H).^{13}C NMR (100.6 MHz, $CDCl_3$) δ 163.8, 154.0, 144.4, 136.6, 127.6, 125.9, 126.3, 98.9, 89.9, 45.1, 39.9, 36.8, 28.7, 24.9, 21.4, 19.4. MS (ESI) *m/z* 285.3 $[M+H]^+$, 307.3 $[M+Na]^+$.

4.1.3.4. 4-(Benzylamino)-6-methyl-1-pentylpyridin-2(1H)-one (7d). Compound **7d** was prepared according to General procedure B, using as reactants intermediate **6c** (100 mg, 0.51 mmol) and benzylamine (1.5 equivalents, 84.1 μL, 0.71 mmol). The reaction was monitored by TLC analysis (DCM/MeOH 96/4; Rf = 0.4). The crude of the reaction was purified by flash chromatography (DCM/MeOH 99/1–98/2), affording the desired product in 31 % yield (45.00 mg, 0.16 mmol).

^{1}H NMR (400 MHz, $CDCl_3$) δ 7.36–7.26 (m, 5H), 5.52 (s, 1H), 5.51 (s, 1H), 4.53 (s, 1H), 4.25 (d, J = 5.4 Hz, 2H), 3.90–3.86 (m, 2H), 2.27 (s, 3H), 1.65–1.63 (m, 2H), 1.36–1.34 (m, 4H), 0.93–0.90 (m, 3H). ^{13}C NMR (100.6 MHz, $CDCl_3$) δ 164.6, 154.5, 144.9, 137.9, 128.8 (2C), 127.6, 127.5 (2C), 99.3, 91.4, 47.0, 43.6, 29.2, 28.8, 22.5, 20.4, 14.0. MS (ESI) *m/z* 285.2 $[M+H]^+$, 307.2 $[M+Na]^+$.

4.1.3.5. 1-Benzyl-6-methyl-4-(pentylamino)pyridin-2(1H)-one (7e). Compound **7e** was prepared according to General procedure B, using as reactants intermediate **6b** (110 mg, 0.51 mmol) and pentylamine (1.5 equivalents, 89.4 μL, 0.77 mmol). The reaction was monitored by TLC analysis (DCM/MeOH 96/4; Rf = 0.4). The crude of the reaction was

purified by flash chromatography (DCM/MeOH 99/1–98/2), affording the desired product in 31 % yield (45.00 mg, 0.16 mmol).

^{1}H NMR (400 MHz, $CDCl_3$) δ 7.27–7.14 (m, 5H), 5.54 (s, 1H), 5.49 (s, 1H), 5.25 (d, J = 5.4 Hz, 2H), 4.30 (s, 1H), 3.10–3.05 (m, 2H), 2.12 (s, 3H), 1.61–1.59 (m, 2H), 1.34–1.27 (m, 4H), 0.93–0.89 (m, 3H). ^{13}C NMR (100.6 MHz, $CDCl_3$) δ 165.0, 155.0, 145.3, 137.7, 128.6 (2C), 126.9, 126.3 (2C), 99.8, 90.0, 46.0, 42.7, 29.2, 28.6, 22.4, 20.5, 14.0. MS (ESI) m/z 285.3 $[M+H]^+$, 307.2 $[M+Na]^+$.

4.1.3.6. 1-Isobutyl-6-methyl-4-((4-(trifluoromethyl)benzyl)amino)pyridin-2(1H)-one (7f). Compound **7f** was prepared according to General procedure B, using as reactants intermediate **6d** (92.00 mg, 0.51 mmol) and 4-(trifluoromethyl)benzylamine (1.5 equivalents, 109.7 μL, 0.77 mmol). The reaction was monitored by TLC analysis (DCM/MeOH 96/4; Rf = 0.4). The crude of the reaction was purified by flash chromatography (DCM/MeOH 99/1–98/2), affording the desired product in 29 % yield (50.00 mg, 0.15 mmol).

^{1}H NMR (400 MHz, $CDCl_3$) δ 7.60 (d, J = 7.8 Hz, 2H), 7.42 (d, J = 7.8 Hz, 2H), 5.53 (s, 1H), 5.46 (s, 1H), 4.59 (s, 1H), 4.36 (d, J = 5.2 Hz, 2H), 3.76–3.74 (m, 2H), 2.27 (s, 3H), 2.20–2.13 (m, 1H), 0.94 (d, J = 6.6 Hz, 6H).^{13}C NMR (100.6 MHz, $CDCl_3$) δ 164.9, 154.2, 145.6, 142.3, 128.0, 127.5 (2C), 125.7 (2C), 125.6, 99.3, 91.8, 50.2, 46.4, 28.1, 20.9, 20.1 (2C). MS (ESI) m/z 339.2 $[M+H]^+$, 361.3 $[M+Na]^+$.

4.1.3.7. 6-Methyl-4-(pentylamino)-1-(4-(trifluoromethyl)benzyl)pyridin-2(1H)-one (7g). Compound **7g** was prepared according to General procedure B, using as reactants intermediate **6f** (100 mg, 0.41 mmol) and pentylamine (3 equivalents, 141.4 μL, 1.22 mmol). The reaction was monitored by TLC analysis (DCM/MeOH 96/4; Rf = 0.4). The crude of the reaction was purified by flash chromatography (DCM/MeOH 98/2), affording the desired product in 68 % yield (83.90 mg, 0.24 mmol).

^{1}H NMR (300 MHz, MeOD-d_4) δ 7.65 (d, 2H, J = 8.26 Hz), 7.32 (d, 2H, J = 7.96 Hz), 5.87 (s, 1H), 5.58 (d, 1H, J = 2.45 Hz), 5.36 (s, 2H), 3.11 (t, 2H, J = 7.04 Hz), 2.20 8s, 3H), 1.66–1.62 (m, 2H), 1.43–1.31 (m, 4H), 0.98–0.92 (m, 3H). ^{13}C NMR (100.6 MHz, $CDCl_3$) δ 163.6, 154.1, 143.9, 140.8, 128.3 (q, $J_{C\text{-}F}$ = 32.20 Hz), 125.5, 124.6, 123.0 (q, $J_{C\text{-}F}$ = 271.64 Hz), 99.0, 88.9, 44.8, 41.7, 28.1, 27.6, 21.3, 19.4, 12.9. MS (ESI) m/z 353.2 $[M+H]^+$.

4.1.3.8. 4-(cyclopentylamino)-6-methyl-1-(4-(trifluoromethyl)benzyl)pyridin-2(1H)-one (7 h). Compound **7h** was prepared according to General procedure B, using as reactants intermediate **6e** (100 mg, 0.35 mmol) and cyclopentamine (3 equivalents, 120.8 μL, 1.22 mmol). The reaction was monitored by TLC analysis (DCM/MeOH 96/4; Rf = 0.4). The crude of the reaction was purified by flash chromatography (DCM/MeOH 98/2), affording the desired product in 37 % yield (45.55 mg, 0.13 mmol).

^{1}H NMR (300 MHz, $CDCl_3$) δ 7.72 (d, 2H, J = 8.23 Hz), 7.31 (d, 2H, J = 8.23 Hz), 5.89 (bs, 1H), 5.44 (bs, 1H), 5.26 (s, 2H), 3.71 (s, 1H), 2.15 (s, 3H), 1.92–1.24 (m, 8H).^{13}C NMR (100.6 MHz, $CDCl_3$) δ 163.6, 153.5, 143.9, 140.8, 128.3 (q, $J_{C\text{-}F}$ = 32.19 Hz), 125.6, 124.6, 121.7, 99.3, 89.6, 52.8, 44.8, 32.2, 22.9, 19.4. MS (ESI) m/z 351.1 $[M+H]^+$.

4.1.3.9. 1-(4-methoxybenzyl)-6-methyl-4-(pentylamino)pyridin-2(1H)-one (7i). Compound **7i** was prepared according to General procedure B, using as reactants intermediate **6f** (100 mg, 0.41 mmol) and pentylamine (3 equivalents, 141.4 μL, 1.22 mmol). The reaction was monitored by TLC analysis (DCM/MeOH 96/4; Rf = 0.4). The crude of the reaction was purified by flash chromatography (DCM/MeOH 97/3), affording the desired product in 15 % yield (21.00 mg, 0.06 mmol).

^{1}H NMR (300 MHz, $CDCl_3$) δ 7.03 (d, 2H, J = 9.96 Hz), 6.74 (d, 2H, J = 6.64 Hz), 5.46 (s, 1H), 5.37 (s, 1H), 5.10 (s, 2H), 3.69 (s, 3H), 3.02-2-98 (m, 2H), 2.07 (s, 3H), 1.53–1.50 (m, 2H), 1.28–1.26 (m, 4H), 0.86–0.82 (m, 3H).^{13}C NMR (100.6 MHz, $CDCl_3$) δ 163.9, 157.6, 153.8, 144.4, 128.8, 126.7, 113.0, 98.6, 89.3, 54.2, 44.5, 41.7, 28.1, 27.7, 21.4, 19.5, 13.0. MS (ESI) m/z 315.2 $[M+H]^+$.

4.1.3.10. 4-(cyclopentylamino)-1-(4-methoxybenzyl)-6-methylpyridin-2(1H)-one (7j). Compound **7j** was prepared according to General procedure B, using as reactants intermediate **6f** (100 mg, 0.41 mmol) and cyclopentamine (3 equivalents, 120.8 μL, 1.22 mmol). The reaction was monitored by TLC analysis (DCM/MeOH 96/4; Rf = 0.4). The crude of the reaction was purified by flash chromatography (DCM/MeOH 97/3), affording the desired product in 32 % yield (6.30 mg, 0.02 mmol).

^{1}H NMR (300 MHz, $CDCl_3$) δ 7.11 (d, 2H, J = 8.50 Hz), 6.83 (d, 2H, J = 8.5 Hz), 5.58 (s, 1H), 5.48 (s, 1H), 5.18 (s, 2H), 4.28 (d, 1H, J = 6.20 Hz), 3.78 (s, 3H), 2.15 (s, 3H), 2.02–1.99 (m, 2H), 1.71–1.63 (m, 4H), 1.51–1.48 (m, 2H).^{13}C NMR (100.6 MHz, $CDCl_3$) δ 164.5, 158.7, 154.7, 145.5, 129.5, 127.8, 114.1, 100.5, 90.1, 55.3, 53.9, 45.8, 33.2, 24.0, 20.5. MS (ESI) m/z 313.1 $[M+H]^+$.

4.1.3.11. 1-(2,3-dimethoxybenzyl)-6-methyl-4-(pentylamino)pyridin-2(1H)-one (7k). Compound **7k** was prepared according to General procedure B, using as reactants intermediate **6g** (100 mg, 0.36 mmol) and pentylamine (3 equivalents, 126.3 μL, 1.09 mmol). The reaction was monitored by TLC analysis (DCM/MeOH 96/4; Rf = 0.4). The crude of the reaction was purified by flash chromatography (DCM/MeOH 98/2–97/3), affording the desired product in 30 % yield (37.17 mg, 0.11 mmol).

^{1}H NMR (300 MHz, $CDCl_3$) δ 6.96 (t, 1H, J = 8.41 Hz), 6.80 (d, 1H, J = 8.41 Hz), 6.50 (d, 1H, J = 8.41 Hz), 5.54 (d, 1H, J = 2.50 Hz), 5.48 (d, 1H, J = 2.05 Hz), 5.32 (s, 2H), 3.89 (s, 3H), 3.87 (s, 3H), 3.11–3.06 (m, 2H), 2.09 (s, 3H), 1.65–1.58 (m, 2H), 1.37–1.33 (m, 4H), 0.94–0.91 (m, 3H).^{13}C NMR (100.6 MHz, $CDCl_3$) δ 165.1, 155.0, 152.4, 145.9, 145.6, 131.6, 124.5, 118.4, 110.9, 99.6, 90.0, 77.1, 76.7, 60.7, 55.7, 42.7, 40.8, 29.2, 28.7, 22.4, 20.2, 14.0. MS (ESI) m/z 345.2 $[M+H]^+$.

4.1.3.12. 6-Methyl-1-pentyl-4-((4-(trifluoromethyl)benzyl)amino)pyridin-2(1H)-one (7l). Compound **7l** was prepared according to General procedure B, using as reactants intermediate **6c** (100 mg, 0.51 mmol) and (4-(trifluoromethyl)phenyl)methanamine (3 equivalents, 220.6 μL, 1.54 mmol). The reaction was monitored by TLC analysis (DCM/MeOH 96/4; Rf = 0.4). The crude of the reaction was purified by flash chromatography (DCM/MeOH 98/2–97/3), affording the desired product in 17 % yield (30 mg, 0.08 mmol).

^{1}H NMR (300 MHz, $CDCl_3$) δ 7.58 (d, 2H, J = 7.77 Hz), 7.41 (d, 2H, J = 7.77 Hz), 5.56 (d, 1H, J = 1.69 Hz), 5.43 (d, 1H, J = 2.21 Hz), 4.84 (bs, 1H), 4.3 (d, 2H, J = 6.67 Hz), 3.89–3.85 (m, 2H), 2.28 (s, 3H), 1.67–1.59 (m, 2H), 1.36–1.32 (m, 4H), 2.96–2.89 (m, 3H).^{13}C NMR (100.6 MHz, $CDCl_3$) δ 164.4, 154.5, 145.2, 142.1, 129.7 (q, $J_{C\text{-}F}$ = 32.6 Hz), 127.4, 125.7, 125.6, 124.1 (q, $J_{C\text{-}F}$ = 271.9 Hz), 99.5, 91.5, 46.3, 43.7, 29.7, 29.1, 28.8, 22.5, 20.4, 14.0. MS (ESI) m/z 353.1 $[M+H]^+$.

4.1.4. General procedure C

In a 10 mL microwave tube, equipped with magnetic stir bar and septum, a mixture of 4-amino-pyridone (5c or **7g**), acetyl chloride (2.5 equivalents), and pyridine (2.5 equivalents) in anhydrous DCM (1.5 mL) was heated at 45 °C for 30 min in the microwave apparatus (maximum power input: 300 W; maximum pressure: 250 psi; power max: OFF; stirring: ON). After cooling to room temperature, the solution was diluted with Ethyl Acetate and washed with $NaHCO_3$ sat. sol. The aqueous phase was then extracted with Ethyl Acetate (3 times), and the collected organic layers washed with BRINE, dried over Na_2SO_4, filtered, and the solvent removed under reduced pressure.

4.1.4.1. N-(6-methyl-2-oxo-1-(4-(trifluoromethyl)benzyl)-1,2-dihydropyridin-4-yl)-N-pentylacetamide (8a). Compound **8a** was synthesized according to the General procedure C, using as starting material compound **7g** (50 mg, 0.14 mmol). The reaction was monitored by TLC analysis (DCM/MeOH 97/3; Rf = 0.4). The crude of the reaction was then purified by flash chromatography (DCM/MeOH 98/2), affording the desired product as yellowish solid in 43 % yield (23.70 mg, 0.06 mmol).

^{1}H NMR (300 MHz, $CDCl_3$) δ 7.62 (d, 2H, J = 8.38 Hz), 7.32 (d, 2H, J = 8.38 Hz), 6.38 (d, 1H, J = 2.12 Hz), 6.00 (s, 1H), 5.40 (s, 1H), 3.68–3.64 (m, 2H), 3.11 (s, 3H), 2.10 (s, 3H), 1.60–1.53 (m, 2H), 1.36–1.27 (m, 4H), 0.90 (t, 3H, J = 7.10 Hz).^{13}C NMR (100.6 MHz, $CDCl_3$) δ 169.2, 164.1, 153.3, 147.2, 140.0, 130.0 (q, $J_{C\text{-}F}$ = 33.56 Hz), 126.9, 125.9, 125.9, 123.9 (q, $J_{C\text{-}F}$ = 274.06 Hz), 114.5, 107.1, 48.4, 46.9, 29.7, 28.9, 27.9, 22.9, 22.4, 20.8, 14.0. MS (ESI) m/z 395.2 $[M+H]^+$.

4.1.4.2. N-(6-methyl-2-oxo-1-(4-(trifluoromethyl)benzyl)-1,2-dihydropyridin-4-yl)-N-(4-(trifluoromethyl)benzyl)acetamide (8b). Compound **8a** was synthesized according to the General procedure C, using as starting material compound **5c** (100 mg, 0.23 mmol). The reaction was monitored by TLC analysis (DCM/MeOH 97/3; Rf = 0.4). The crude of the reaction was then purified by flash chromatography (DCM/MeOH 98/2), affording the desired product as yellowish solids in 51 % yield (46.00 mg, 0.12 mmol).

^{1}H NMR (300 MHz, $CDCl_3$) δ 7.51–7.48 (m, 4H), 7.27 (d, 2H, J = 8.37 Hz), 7.16 (d, 2H, J = 8.37 Hz), 6.18 (d, 1H, J = 2.30 Hz), 5.83 (s, 1H), 5.26 (s, 2H), 4.85 (s, 2H), 2.18 (s, 3H), 2.09 (s, 3H).^{13}C NMR (100.6 MHz, $CDCl_3$) δ 168.6, 162.7, 151.7, 146.5, 139.6, 138.7, 128.9 (q, $J_{C\text{-}F}$ = 32.83 Hz), 128.8 (q, $J_{C\text{-}F}$ = 32.51 Hz), 126.9, 125.7, 124.8, 124.8, 124.6, 124.5, 122.9 (q, $J_{C\text{-}F}$ = 272.08 Hz), 121.8 (q, $J_{C\text{-}F}$ = 272.08 Hz), 113.1, 105.4, 50.3, 45.8, 21.7, 19.7. MS (ESI) m/z 483.1 $[M+H]^+$.

4.1.5. Cell cultures

HepG2 cell line was cultured in 100 mm Petri dishes in Modified Eagle's Medium (MEM) supplemented with 10 % Fetal Bovine Serum (FBS), 1 % penicillin/streptomycin solution (10.000U/mL and 10 mg/mL, respectively), 1 % L-glutamine 200 mM and 1 % non-essential amino acids 100X solution. Cells were maintained at 37 °C, 95 % humidity and 5 % CO_2 and subcultured at 80 % confluency. All cell culture reagents and plastic supplies were purchased from EuroClone (Milan, Italy). HepG2 overexpressing human PCSK9-FLAG tag were generated by the means of HEK293-Phoenix (φNX-A) cells as previously described [50], using empty pBMN-IRES-puromycin vector or the same vector carrying human PCSK9 coding sequence under CMV promoter to generate, respectively, HepG2 and HepG2 PCSK9-FLAG cells.

Simvastatin (Merck Sharp & Dohme Research Laboratories, Readington, NJ, USA) was dissolved in 0.1 M NaOH and the pH was adjusted to 7.4, then the solution was sterilized by filtration.

Testing compounds (**1**–**4**; **5a-f**, **7a-l**, **8a,b**) were provided in a powder form. They were dissolved in dimethyl sulfoxide (DMSO, Sigma Aldrich) to a concentration of 80 mM. To maintain the quality of the compounds, they were stored at −20 °C.

4.1.6. Sulphorodamine B cell viability assay

Cellular toxicity of the MR compounds was assessed using sulphorodamine (SRB) assay according the protocol established by Shehan et al. [51]. 8000 cells/well were seeded in a 96 well-tray in 100μl/well of complete medium. The following day the medium was replaced by fresh media containing 0.4 % FBS and treatments or DMSO as control. After 24 h of incubation, SRB assay was performed and absorbances measured at 570 nm with Victor Nivo multiplate reader by PerkinElmer.

4.1.7. Western blotting

Cells were lysed in lysis buffer containing 1 % NP-40, 150 mM NaCl and 50 mM Tris-HCl at pH 7.5. Protein concentration was assessed by BCA assays (SERVA), accordingly to manufacturer's instructions. 25 μg total protein extract was loaded and separated on 4–20 % SDS-Page gel (Bio-Rad) under denaturing and reducing conditions. Proteins were then transferred onto a nitrocellulose membrane by using the Trans-Blot® Turbo™ Transfer System (Bio-Rad). Blocking solution is made of 5 % non-fat dried milk in tris-buffered saline containing 0.2 % of tween 20 (TBST20). All the primary antibodies were diluted in blocking solution and incubated overnight at 4 °C in agitation. Horseradish peroxidase (HPR) conjugated secondary antibodies were diluted in blocking solution and membranes were incubate 2 h at room temperature (RT) in agitation.

Luminescence signals were acquired with c400 Azure Molecular Imager (Aurogene). Quantitative densitometric analysis was performed with ImageLab™ (Version 6.0.1, BIO-RAD) software. PCSK9 antibody was from Abcam (cod. ab181142; dilution 1:1000), LDLR antibody was from was from GeneTex (cod. GTX132860; dilution 1:1000), beta-actin antibody was from GeneTex (cod. GTX109639; dilution 1:5000), anti-rabbit secondary antibody was from Jackson Immuno Research (cod. 113-036-045, dilution 1:5000).

4.1.8. Reverse transcription and quantitative PCR (RT-qPCR)

Total RNA was extracted using the iScript™ RT-qPCR Sample Prep reagent (Bio-Rad), according to the manufacturer's instructions. QuantiNova SYBR Green RT-PCR Kit (QIAGEN) was used for qPCR, along with specific primers for 18S (FWD 5′-CGGCTACCACATCCACGGAA-3′, REV 5′-CCTGAATTGTTATTTTTCGTCACTACC-3′) PCSK9 (FWD 5′-CCTGCGCGTGCTCAACT-3′, REV 5′-GCTGGCTTTTCCGAATAAACTC-3′), LDLR (FWD 5′- TCTATGGAAGAACTGGCGGC-3′, REV 5′-ACCATCTGTCTCGAGGGGTA-3′) FAS (FWD 5′-GCAAATTC-GACCTTTCTCA-3′, REV 5' - GGACCCCGTGGAATGTCA-3′), HMG-CoAR (FWD 5′- CTTGTGTGTCCTTGGTATTAGAGCTT-3′, REV 5′-GCTGAGCTGCCAAATTGGA-3′).

The analyses were performed with the CFX96 Touch Real-Time PCR Detection System (Bio-Rad) with cycling conditions of 50 °C for 10 min, 95 °C for 2 min, and a repetition of 40 cycles at 95 °C for 5 s followed by 10 s at 60 °C. The data were expressed as Ct values and used for relative quantification of targets with ΔΔCt calculations. The ΔΔCt values were determined by multiplying the ratio value between the efficiency of specific primers and housekeeping 18S. The efficiency was calculated as ((10ˆ(−1/slope)) - 1) x 100.

4.1.9. ELISA assay for PCSK9

To detect the secreted amount of PCSK9 from HepG2 cells, the Human Proprotein Convertase 9/PCSK9 DuoSet ELISA (Biotechne) was used according to the manufacturer's instructions using conditioned media. Conditioned media were collected, centrifuged 15000 rpm for 10 min and diluted according to the manufacturer's instructions. Absorbance at 450 nm was obtained with VICTOR Nivo Multimode Microplate Reader (PerkinElmer).

4.1.10. Luciferase reported promoter activities assay

The plasmid pGL3-PCSK9-D4 contains the 5′ flanking region of the PCSK9 gene from −440 to −94, relative to the ATG start codon as previously described [52]. To measure the PCSK9 promoter activity, HepG2 cells were seeded in 48 well plates at a density of 8×10^5 cells per well. On the next day, cells were transiently transfected with pGL3-PCSK9-D4 or pGL3-PCSK9-SREmut or pGL3-PCSK9-HNFmut and, 48 h post transfection, cells were treated with simvastatin or compound **1** for an additional 24 h. Luciferase activities were measured by using Neolite reagent (PerkinElmer, Milan, Italy) according to manufacturer's instructions.

4.1.11. Statistical analysis

Data are expressed as mean ± standard deviation. To compare differences between two conditions, p values were determined by Student's t-test using GraphPad® Software v8.2.1 for Windows. Otherwise, differences between treatment groups were evaluated by one-way ANOVA. A probability value of $p < 0.05$ was considered statistically significant.

4.1.12. In vivo experiment

4.1.12.1. Animals. A total of 17 male three months of age C57Bl6/J

mice (26–30g) were randomly divided into three experimental groups. The first group was assigned to serve as control (Vehicle) and received 100 % Diethylene Glycol Monoethyl Ether (Transcutol), the second and the third ones received SBC-115076 (4 mg/kg), a well-known PCSK9 inhibitor, or **5c** (40 mg/kg) respectively. All drugs and vehicle were subcutaneously injected (SQ-inj) for seven days. Mice were kept in a conventional animal facility with controlled temperature (20–24 °C) and humidity (60 %) on a light/dark cycle of 12 h. Food and water were available *ad libitum* and body weight was recorded throughout the entire observation period. All animal procedures were approved by the Committee on Animal Health and Care of the University of Modena and Reggio Emilia (protocol number: n° 511/2019-PR) and conducted following National Institutes of Health guidelines.

4.1.12.2. Behavioral screening and analysis. Behavioral tests were performed by an operator unaware of the treatment to avoid bias. Animal behavior was conducted in a sound-proof room, recorded and automatically analyzed with ANY-maze Video Tracking system (Stoelting).

For three days, after body weight recording, all mice underwent an Open Field task [53] to evaluate general motor activity and anxiety (Basal Day1–3). The animal was placed in the centre of an open wooden chamber (50 × 50 × 40 cm) and allowed to explore for 10 min freely. Travelled distance and speed were automatically recorded. On the third day, after basal activity recordings, all animals received a 50 μl SQ-inj according to the experimental group and for six consecutive days.

For testing the effects of subacute treatments, all animals were subjected to a Shirpa modified test [54]. This standard test is used to evaluate general phenotype, such as hence muscle, sensory, cerebellar, and neuropsychiatric functions *in vivo* and consists in the observation of spontaneous mouse behavior in its home cage for 3 min. The analysis was carried out according to the parameters given in Table 2. All data are shown as mean ± standard error of the mean (SEM) and were analyzed by two-way repeated measures analysis of variance (ANOVA) using the statistical package SPSS (version 26). Differences were considered significant with p-value <0.05, with $p < 0.05$ *; $p < 0.01$ **; $p < 0.001$ ***.

4.1.12.3. Sacrifice and serum collection. At the end of the experiment, after 6 h after the last SQ-inj mice were sacrificed under deep anesthesia with isoflurane and blood samples was obtained through a retro-orbital bleeding. The blood was collected in ethylenediamine tetra acetic acid (EDTA) coated tubes and centrifuged at 3000 rpm at 4 °C for 10 min. The surnatant was collected and stored at −80 until use. For each animal, also brain and peripheral organs were dissected out and immediately frozen in liquid nitrogen. Plasma total cholesterol was determined by colorimetric assay (ABX Penta, cholesterol assay). PCSK9 was determined with Quantikine® Mouse Proprotein Convertase 9 ELISA assay (R&D Systems, Catalog #: MPC900). ALT detection on mouse serum samples was performed using mouse Alanine Aminotransferase (ALT) ELISA kit from MyBiosource (catalog #MBS264717) following manufacturer procedure.

Table 2
Behavioral observation and score for the assessment of the general animal welfare.

		Score		
		0	1	2
Behavioral observations	**general activity**	inactive	active	hyperactive
	tremors	inexistent	available	
	eyelid opening	open	closed	
	fur coat	carefull	bristly	
	vibrissae	available	inexistent	
	movement			
	defecation	available	inexistent	

4.1.12.4. Total RNA extraction, reverse transcription, and real time polymerase chain reaction. The liver was lysed by mechanical disruption in Trizol reagent (Qiagen), homogenized following the procedure provided by the manufacturer (RNeasy Plus Mini Kit, Qiagen) and processed for quantitative PCR (qPCR) as previously described [55]. Isolated mRNA was reverse transcribed to cDNA using random hexamers and M-MLV Reverse Transcriptase (Promega Corporation) following the instructions provided by the manufacturer. Samples were heated at 70 °C for 5 min to eliminate any secondary structures, then incubated at 23 °C for 10 min, 1 h at 37 °C, and 5 min at 95 °C before being chilled at 4 °C using a thermocycler T Gradient (SimpliAmp, Applied Biosystem). The amount of cDNA was quantified with iTaq Universal SYBR Green Supermix (Bio-Rad) using a Bio-Rad RT-PCR iCycler. Each PCR reaction was performed in triplicate using 300 nM of each primer (Table 3), 10 μL of iTaq Universal SYBR Green Supermix (Bio-Rad), cDNA and nuclease-free water with the following cycling parameters: 2 min at 95 °C and 40 cycles of 5 min at 95 °C and 30 s at 60 °C, followed by 5 s at 95 °C and 65°–95° melting curve analysis.

4.1.12.5. PCR product and statistical analyses. For gene expression analysis, mRNA levels of *Pcsk9* gene target were normalized to *Gapdh* reference gene. For quantitative evaluation of changes, the comparative ΔΔCt method was performed, using as calibrator the average levels of expression of Vehicle mice. Statistical comparisons were performed using the one-way ANOVA.

4.1.12.6. Histological analysis. Liver samples were fixed in 4 % paraformaldehyde (PFA), incubated overnight at +4 °C in PBS/20 % sucrose sterile solution and embedded in Tissue-Tek OCT (Kaltek, Padua, Italy). Samples were processed for optical microscopy by collecting 7 μm thickness sections using a cryostat. Sections were furtherly fixed with 10 % Neutral Buffered Formalin, extensively washed in PBS and then subjected to hematoxylin/eosin staining. Slides were mounted with Eukitt® Quick-hardening mounting medium (Sigma-Aldrich, St. Louis, MO, USA), and coverslips were sealed. Images were acquired with a ZEISS AXIOVERT 200 microscope and visually examined by two different operators.

CRediT authorship contribution statement

Lisa Giannessi: Writing – original draft, Methodology, Investigation, Data curation. **Maria Giovanna Lupo:** Methodology, Investigation, Data curation. **Ilaria Rossi:** Investigation, Data curation. **Maria Grazia Martina:** Investigation, Data curation. **Antonietta Vilella:** Investigation, Data curation. **Martina Bodria:** Investigation, Data curation. **Daniela Giuliani:** Investigation, Data curation. **Francesca Zimetti:** Investigation, Data curation. **Ilaria Zanotti:** Investigation, Data curation. **Francesco Potì:** Investigation, Data curation. **Franco Bernini:** Supervision, Investigation, Data curation. **Nicola Ferri:** Writing – review & editing, Writing – original draft, Supervision, Project administration, Methodology, Investigation, Funding acquisition, Data curation. **Marco Radi:** Writing – review & editing, Writing – original draft, Supervision, Resources, Project administration, Methodology, Investigation, Funding acquisition, Formal analysis, Data curation, Conceptualization.

Table 3
List of primers used for ex-vivo qPCR experiments.

Transcript	NCBI Ref Seq	Primer	sequence (5′- 3′)
Gapdh	NM_008084.3	Fw	CAAGGTCATCCATGACAACTTTG
		Rv	GGGCCATCCACAGTCTTCTG
Pcsk9	NM_153565	Fw	AACCTGGAGCGAATTATCCCA
		Rv	TTGAAGTCGGTGATGGTGACC

Declaration of competing interest

The authors declare that they have no known competing financial interests or personal relationships that could have appeared to influence the work reported in this paper.

Data availability

Data will be made available on request.

Acknowledgment

This work was supported by the University of Parma (Fondo di Ateneo per la Ricerca Locale 2021 to FB and MR) and by Progetto Dipartimenti di Eccellenza 2023–2027 (to DipALIFAR). MR also thanks Aleix Bassas for excellent technical assistance.

Appendix A. Supplementary data

Supplementary data to this article can be found online at https://doi.org/10.1016/j.ejmech.2023.116063.

References

[1] C. Macchi, N. Ferri, C.R. Sirtori, A. Corsini, M. Banach, M. Ruscica, Proprotein convertase subtilisin/kexin type 9: a view beyond the canonical cholesterol-lowering impact, Am. J. Pathol. 191 (2021) 1385–1397, https://doi.org/10.1016/j.ajpath.2021.04.016.

[2] N.G. Seidah, A. Prat, The biology and therapeutic targeting of the proprotein convertases, Nat. Rev. Drug Discov. 11 (2012) 367–383, https://doi.org/10.1038/nrd3699.

[3] N. He, Q. Li, C. Wu, Z. Ren, Y. Gao, L. Pan, M. Wang, H. Wen, Z. Jiang, Z. Tang, L. Liu, Lowering serum lipids via PCSK9-targeting drugs: current advances and future perspectives, Acta Pharmacol. Sin. 38 (2017) 301–311, https://doi.org/10.1038/aps.2016.134.

[4] S.E. Nissen, E. Stroes, R.E. Dent-Acosta, R.S. Rosenson, S.J. Lehman, N. Sattar, D. Preiss, E. Bruckert, R. Ceška, N. Lepor, C.M. Ballantyne, I. Gouni-Berthold, M. Elliott, D.M. Brennan, S.M. Wasserman, R. Somaratne, R. Scott, E.A. Stein, For the GAUSS-3 investigators, efficacy and tolerability of evolocumab vs ezetimibe in patients with muscle-related statin intolerance: the GAUSS-3 randomized clinical trial, JAMA 315 (2016) 1580, https://doi.org/10.1001/jama.2016.3608.

[5] M.S. Sabatine, R.P. Giugliano, S.D. Wiviott, F.J. Raal, D.J. Blom, J. Robinson, C. M. Ballantyne, R. Somaratne, J. Legg, S.M. Wasserman, R. Scott, M.J. Koren, E. A. Stein, Efficacy and safety of evolocumab in reducing lipids and cardiovascular events, N. Engl. J. Med. 372 (2015) 1500–1509, https://doi.org/10.1056/NEJMoa1500858.

[6] B.M. Everett, R.J. Smith, W.R. Hiatt, Reducing LDL with PCSK9 inhibitors — the clinical benefit of lipid drugs, N. Engl. J. Med. 373 (2015) 1588–1591, https://doi.org/10.1056/NEJMp1508120.

[7] G. Dubuc, A. Chamberland, H. Wassef, J. Davignon, N.G. Seidah, L. Bernier, A. Prat, Statins upregulate *PCSK9*, the gene encoding the proprotein convertase neural apoptosis-regulated convertase-1 implicated in familial hypercholesterolemia, ATVB 24 (2004) 1454–1459, https://doi.org/10.1161/01.ATV.0000134621.14315.43.

[8] E. Gallego-Colon, A. Daum, C. Yosefy, Statins and PCSK9 inhibitors: a new lipid-lowering therapy, Eur. J. Pharmacol. 878 (2020), 173114, https://doi.org/10.1016/j.ejphar.2020.173114.

[9] K.K. Ray, R.S. Wright, D. Kallend, W. Koenig, L.A. Leiter, F.J. Raal, J.A. Bisch, T. Richardson, M. Jaros, P.L.J. Wijngaard, J.J.P. Kastelein, Two phase 3 trials of inclisiran in patients with elevated LDL cholesterol, N. Engl. J. Med. 382 (2020) 1507–1519, https://doi.org/10.1056/NEJMoa1912387.

[10] N. Wang, A.R. Tall, A new approach to PCSK9 therapeutics, Circ. Res. 120 (2017) 1063–1065, https://doi.org/10.1161/CIRCRESAHA.117.310610.

[11] T. Nishikido, K.K. Ray, Non-antibody approaches to proprotein convertase subtilisin kexin 9 inhibition: siRNA, antisense oligonucleotides, adnectins, vaccination, and new attempts at small-molecule inhibitors based on new discoveries, Front. Cardiovasc. Med. 5 (2019) 199, https://doi.org/10.3389/fcvm.2018.00199.

[12] N. Kuzmich, E. Andresyuk, Y. Porozov, V. Tarasov, M. Samsonov, N. Preferanskaya, V. Veselov, R. Alyautdin, PCSK9 as a target for development of a new generation of hypolipidemic drugs, Molecules 27 (2022) 434, https://doi.org/10.3390/molecules27020434.

[13] S. Ahamad, S. Mathew, W.A. Khan, K. Mohanan, Development of small-molecule PCSK9 inhibitors for the treatment of hypercholesterolemia, Drug Discov. Today 27 (2022) 1332–1349, https://doi.org/10.1016/j.drudis.2022.01.014.

[14] S. Xu, S. Luo, Z. Zhu, J. Xu, Small molecules as inhibitors of PCSK9: current status and future challenges, Eur. J. Med. Chem. 162 (2019) 212–233, https://doi.org/10.1016/j.ejmech.2018.11.011.

[15] M. Stucchi, G. Grazioso, C. Lammi, S. Manara, C. Zanoni, A. Arnoldi, G. Lesma, A. Silvani, Disrupting the PCSK9/LDLR protein–protein interaction by an imidazole-based minimalist peptidomimetic, Org. Biomol. Chem. 14 (2016) 9736–9740, https://doi.org/10.1039/C6OB01642A.

[16] C. Lammi, J. Sgrignani, A. Arnoldi, G. Lesma, C. Spatti, A. Silvani, G. Grazioso, Computationally driven structure optimization, synthesis, and biological evaluation of imidazole-based proprotein convertase subtilisin/kexin 9 (PCSK9) inhibitors, J. Med. Chem. 62 (2019) 6163–6174, https://doi.org/10.1021/acs.jmedchem.9b00402.

[17] J. Taechalertpaisarn, B. Zhao, X. Liang, K. Burgess, Small molecule inhibitors of the PCSK9·LDLR interaction, J. Am. Chem. Soc. 140 (2018) 3242–3249, https://doi.org/10.1021/jacs.7b09360.

[18] T.J. Tucker, M.W. Embrey, C. Alleyne, R.P. Amin, A. Bass, B. Bhatt, E. Bianchi, D. Branca, T. Bueters, N. Buist, S.N. Ha, M. Hafey, H. He, J. Higgins, D.G. Johns, A. D. Kerekes, K.A. Koeplinger, J.T. Kuethe, N. Li, B. Murphy, P. Orth, S. Salowe, A. Shahripour, R. Tracy, W. Wang, C. Wu, Y. Xiong, H.J. Zokian, H.B. Wood, A. Walji, A series of novel, highly potent, and orally bioavailable next-generation tricyclic peptide PCSK9 inhibitors, J. Med. Chem. 64 (2021) 16770–16800, https://doi.org/10.1021/acs.jmedchem.1c01599.

[19] D.G. Johns, L.-C. Campeau, P. Banka, A. Bautmans, T. Bueters, E. Bianchi, D. Branca, P.G. Bulger, I. Crevecoeur, F.-X. Ding, R.M. Garbaccio, E.D. Guetschow, Y. Guo, S.N. Ha, J.M. Johnston, H. Josien, E.A. Kauh, K.A. Koeplinger, J.T. Kuethe, E. Lai, C.L. Lanning, A.Y.H. Lee, L. Li, A.G. Nair, E.A. O'Neill, S.A. Stoch, D. A. Thaisrivongs, T.J. Tucker, P. Vachal, K. van Dyck, F.P. Vanhoutte, B. Volckaert, D.G. Wolford, A. Xu, T. Zhao, D. Zhou, S. Zhou, X. Zhu, H.J. Zokian, A. Walji, H. B. Wood, Orally bioavailable macrocyclic peptide that inhibits binding of PCSK9 to the low density lipoprotein receptor, Circulation (2023), https://doi.org/10.1161/CIRCULATIONAHA.122.063372.

[20] W.L. Petrilli, G.C. Adam, R.S. Erdmann, P. Abeywickrema, V. Agnani, X. Ai, J. Baysarowich, N. Byrne, J.P. Caldwell, W. Chang, E. DiNunzio, Z. Feng, R. Ford, S. Ha, Y. Huang, B. Hubbard, J.M. Johnston, M. Kavana, J.-M. Lisnock, R. Liang, J. Lu, Z. Lu, J. Meng, P. Orth, O. Palyha, G. Parthasarathy, S.P. Salowe, S. Sharma, J. Shipman, S.M. Soisson, A.M. Strack, H. Youm, K. Zhao, D.L. Zink, H. Zokian, G. H. Addona, K. Akinsanya, J.R. Tata, Y. Xiong, J.E. Imbriglio, From screening to targeted degradation: strategies for the discovery and optimization of small molecule ligands for PCSK9, Cell Chem. Biol. 27 (2020) 32–40, https://doi.org/10.1016/j.chembiol.2019.10.002, e3.

[21] M.-Q. Qiao, Y. Li, Y.-X. Yang, C.-X. Pang, Y.-T. Liu, C. Bian, L. Wang, X.-F. Chen, B. Hong, Structure-activity relationship and biological evaluation of xanthine derivatives as PCSK9 inhibitors for the treatment of atherosclerosis, Eur. J. Med. Chem. 247 (2023), 115047, https://doi.org/10.1016/j.ejmech.2022.115047.

[22] D.N. Petersen, J. Hawkins, W. Ruangsiriluk, K.A. Stevens, B.A. Maguire, T. N. O'Connell, B.N. Rocke, M. Boehm, R.B. Ruggeri, T. Rolph, D. Hepworth, P. M. Loria, P.A. Carpino, A small-molecule anti-secretagogue of PCSK9 targets the 80S ribosome to inhibit PCSK9 protein translation, Cell Chem. Biol. 23 (2016) 1362–1371, https://doi.org/10.1016/j.chembiol.2016.08.016.

[23] N.G. Lintner, K.F. McClure, D. Petersen, A.T. Londregan, D.W. Piotrowski, L. Wei, J. Xiao, M. Bolt, P.M. Loria, B. Maguire, K.F. Geoghegan, A. Huang, T. Rolph, S. Liras, J.A. Doudna, R.G. Dullea, J.H.D. Cate, Selective stalling of human translation through small-molecule engagement of the ribosome nascent chain, PLoS Biol. 15 (2017), e2001882, https://doi.org/10.1371/journal.pbio.2001882.

[24] A.T. Londregan, L. Wei, J. Xiao, N.G. Lintner, D. Petersen, R.G. Dullea, K. F. McClure, M.W. Bolt, J.S. Warmus, S.B. Coffey, C. Limberakis, J. Genovino, B. A. Thuma, K.D. Hesp, G.E. Aspnes, B. Reidich, C.T. Salatto, J.R. Chabot, J.H. D. Cate, S. Liras, D.W. Piotrowski, Small molecule proprotein convertase subtilisin/kexin type 9 (PCSK9) inhibitors: hit to lead optimization of systemic agents, J. Med. Chem. 61 (2018) 5704–5718, https://doi.org/10.1021/acs.jmedchem.8b00650.

[25] W. Li, F.R. Ward, K.F. McClure, S.T.-L. Chang, E. Montabana, S. Liras, R. Dullea, J. H.D. Cate, Structural basis for selective stalling of human ribosome nascent chain complexes by a drug-like molecule, Biophysics (2018), https://doi.org/10.1101/315325.

[26] C. Barale, E. Melchionda, A. Morotti, I. Russo, PCSK9 biology and its role in atherothrombosis, Indian J. Manag. Sci. 22 (2021) 5880, https://doi.org/10.3390/ijms22115880.

[27] D. Cunningham, D.E. Danley, K.F. Geoghegan, M.C. Griffor, J.L. Hawkins, T. A. Subashi, A.H. Varghese, M.J. Ammirati, J.S. Culp, L.R. Hoth, M.N. Mansour, K. M. McGrath, A.P. Seddon, S. Shenolikar, K.J. Stutzman-Engwall, L.C. Warren, D. Xia, X. Qiu, Structural and biophysical studies of PCSK9 and its mutants linked to familial hypercholesterolemia, Nat. Struct. Mol. Biol. 14 (2007) 413–419, https://doi.org/10.1038/nsmb1235.

[28] D.C. Swinney, Phenotypic drug discovery: history, evolution, future, in: B. Isherwood, A. Augustin (Eds.), Phenotypic Drug Discovery, The Royal Society of Chemistry, 2020, pp. 1–19, https://doi.org/10.1039/9781839160721-00001.

[29] D.C. Swinney, J.A. Lee, Recent advances in phenotypic drug discovery 9 (2020) 944, https://doi.org/10.12688/f1000research.25813.1. F1000Res.

[30] M.P. Adorni, F. Zimetti, M.G. Lupo, M. Ruscica, N. Ferri, Naturally occurring PCSK9 inhibitors, Nutrients 12 (2020) 1440, https://doi.org/10.3390/nu12051440.

[31] D.N. Petersen, J. Hawkins, W. Ruangsiriluk, K.A. Stevens, B.A. Maguire, T. N. O'Connell, B.N. Rocke, M. Boehm, R.B. Ruggeri, T. Rolph, D. Hepworth, P. M. Loria, P.A. Carpino, A small-molecule anti-secretagogue of PCSK9 targets the 80S ribosome to inhibit PCSK9 protein translation, Cell Chem. Biol. 23 (2016) 1362–1371, https://doi.org/10.1016/j.chembiol.2016.08.016.

[32] H. Xie, K. Yang, G.N. Winston-McPherson, D.S. Stapleton, M.P. Keller, A.D. Attie, K. A. Smith, W. Tang, From methylene bridged diindole to carbonyl linked

benzimidazoleindole: development of potent and metabolically stable PCSK9 modulators, Eur. J. Med. Chem. 206 (2020), 112678, https://doi.org/10.1016/j.ejmech.2020.112678.
[33] G.N. Winston-McPherson, H. Xie, K. Yang, X. Li, D. Shu, W. Tang, Discovery of 2,3′-diindolylmethanes as a novel class of PCSK9 modulators, Bioorg. Med. Chem. Lett 29 (2019) 2345–2348, https://doi.org/10.1016/j.bmcl.2019.06.014.
[34] A. Sadri, Is target-based drug discovery efficient? Discovery and "off-target" mechanisms of all drugs, J. Med. Chem. 66 (2023) 12651–12677, https://doi.org/10.1021/acs.jmedchem.2c01737.
[35] J. Vucicevic, T. Srdic-Rajic, M. Pieroni, J.M.M. Laurila, V. Perovic, S. Tassini, E. Azzali, G. Costantino, S. Glisic, D. Agbaba, M. Scheinin, K. Nikolic, M. Radi, N. Veljkovic, A combined ligand- and structure-based approach for the identification of rilmenidine-derived compounds which synergize the antitumor effects of doxorubicin, Bioorg. Med. Chem. 24 (2016) 3174–3183, https://doi.org/10.1016/j.bmc.2016.05.043.
[36] F. Aiello, G. Carullo, F. Giordano, E. Spina, A. Nigro, A. Garofalo, S. Tassini, G. Costantino, P. Vincetti, A. Bruno, M. Radi, Identification of breast cancer inhibitors specific for G protein-coupled estrogen receptor (GPER)-Expressing cells, ChemMedChem 12 (2017) 1279–1285, https://doi.org/10.1002/cmdc.201700145.
[37] B. Dong, H. Li, A.B. Singh, A. Cao, J. Liu, Inhibition of PCSK9 transcription by berberine involves down-regulation of hepatic HNF1α protein expression through the ubiquitin-proteasome degradation pathway, J. Biol. Chem. 290 (2015) 4047–4058, https://doi.org/10.1074/jbc.M114.597229.
[38] B. Dong, A.B. Singh, V.R. Shende, J. Liu, Hepatic HNF1 transcription factors control the induction of PCSK9 mediated by rosuvastatin in normolipidemic hamsters, Int. J. Mol. Med. 39 (2017) 749–756, https://doi.org/10.3892/ijmm.2017.2879.
[39] Y.-J. Jia, R.-X. Xu, J. Sun, Y. Tang, J.-J. Li, Enhanced circulating PCSK9 concentration by berberine through SREBP-2 pathway in high fat diet-fed rats, J. Transl. Med. 12 (2014) 103, https://doi.org/10.1186/1479-5876-12-103.
[40] H. Li, B. Dong, S.W. Park, H.-S. Lee, W. Chen, J. Liu, Hepatocyte nuclear factor 1α plays a critical role in PCSK9 gene transcription and regulation by the natural hypocholesterolemic compound berberine, J. Biol. Chem. 284 (2009) 28885–28895, https://doi.org/10.1074/jbc.M109.052407.
[41] V.R. Shende, M. Wu, A.B. Singh, B. Dong, C.F.K. Kan, J. Liu, Reduction of circulating PCSK9 and LDL-C levels by liver-specific knockdown of HNF1α in normolipidemic mice, JLR (J. Lipid Res.) 56 (2015) 801–809, https://doi.org/10.1194/jlr.M052969.
[42] G. Dubuc, A. Chamberland, H. Wassef, J. Davignon, N.G. Seidah, L. Bernier, A. Prat, Statins upregulate PCSK9, the gene encoding the proprotein convertase neural apoptosis-regulated convertase-1 implicated in familial hypercholesterolemia, Arterioscler. Thromb. Vasc. Biol. 24 (2004) 1454–1459, https://doi.org/10.1161/01.ATV.0000134621.14315.43.
[43] M. Ruscica, C. Ricci, C. Macchi, P. Magni, R. Cristofani, J. Liu, A. Corsini, N. Ferri, Suppressor of cytokine signaling-3 (SOCS-3) induces proprotein convertase subtilisin kexin type 9 (PCSK9) expression in hepatic HepG2 cell line, J. Biol. Chem. 291 (2016) 3508–3519, https://doi.org/10.1074/jbc.M115.664706.
[44] C. Macchi, M.F. Greco, M. Botta, P. Sperandeo, P. Dongiovanni, L. Valenti, A.F. G. Cicero, C. Borghi, M.G. Lupo, S. Romeo, A. Corsini, P. Magni, N. Ferri, M. Ruscica, Leptin, resistin, and proprotein convertase subtilisin/kexin type 9: the role of STAT3, Am. J. Pathol. 190 (2020) 2226–2236, https://doi.org/10.1016/j.ajpath.2020.07.016.
[45] M.G. Lupo, C. Macchi, S. Marchianò, R. Cristofani, M.F. Greco, S. Dall'Acqua, H. Chen, C.R. Sirtori, A. Corsini, M. Ruscica, N. Ferri, Differential effects of red yeast rice, Berberis aristata and Morus alba extracts on PCSK9 and LDL uptake, Nutr. Metabol. Cardiovasc. Dis. 29 (2019) 1245–1253, https://doi.org/10.1016/j.numecd.2019.06.001.
[46] H.J. Jeong, H.-S. Lee, K.-S. Kim, Y.-K. Kim, D. Yoon, S.W. Park, Sterol-dependent regulation of proprotein convertase subtilisin/kexin type 9 expression by sterol-regulatory element binding protein-2, JLR (J. Lipid Res.) 49 (2008) 399–409.
[47] H. Li, B. Dong, S.W. Park, H.-S. Lee, W. Chen, J. Liu, Hepatocyte nuclear factor 1alpha plays a critical role in PCSK9 gene transcription and regulation by the natural hypocholesterolemic compound berberine, J. Biol. Chem. 284 (2009) 28885–28895, https://doi.org/10.1074/jbc.M109.052407.
[48] S. S. Abdel-Meguid, N. Elshourbagy, H. Meyers, S. A. Mousa, Anti-proprotein Convertase Subtilisin Kexin Type 9 (Anti-PCSK9) Compounds and Methods of Using the Same in the Treatment And/or Prevention of Cardiovascular Diseases. WO2014150326A1.
[49] B.J. Evison, J.T. Palmer, G. Lambert, H. Treutlein, J. Zeng, B. Nativel, K. Chemello, Q. Zhu, J. Wang, Y. Teng, W. Tang, Y. Xu, A.K. Rathi, S. Kumar, A.K. Suchowerska, J. Parmar, I. Dixon, G.E. Kelly, J. Bonnar, A small molecule inhibitor of PCSK9 that antagonizes LDL receptor binding via interaction with a cryptic PCSK9 binding groove, Bioorg. Med. Chem. 28 (2020), 115344, https://doi.org/10.1016/j.bmc.2020.115344.
[50] K.J. Garton, N. Ferri, E.W. Raines, Efficient expression of exogenous genes in primary vascular cells using IRES-based retroviral vectors, Biotechniques 32 (830) (2002) 832, https://doi.org/10.2144/02324rr01, 834 passim.
[51] P. Skehan, R. Storeng, D. Scudiero, A. Monks, J. McMahon, D. Vistica, J.T. Warren, H. Bokesch, S. Kenney, M.R. Boyd, New colorimetric cytotoxicity assay for anticancer-drug screening, J. Natl. Cancer Inst. 82 (1990) 1107–1112, https://doi.org/10.1093/jnci/82.13.1107.
[52] H. Li, B. Dong, S.W. Park, H.-S. Lee, W. Chen, J. Liu, Hepatocyte nuclear factor 1alpha plays a critical role in PCSK9 gene transcription and regulation by the natural hypocholesterolemic compound berberine, J. Biol. Chem. 284 (2009) 28885–28895, https://doi.org/10.1074/jbc.M109.052407.
[53] D.C. Rogers, J. Peters, J.E. Martin, S. Ball, S.J. Nicholson, A.S. Witherden, M. Hafezparast, J. Latcham, T.L. Robinson, C.A. Quilter, E.M. Fisher, SHIRPA, a protocol for behavioral assessment: validation for longitudinal study of neurological dysfunction in mice, Nuerosci. Lett. 306 (2001) 89–92, https://doi.org/10.1016/s0304-3940(01)01885-7.
[54] A.K. Krauter, P.C. Guest, Z. Sarnyai, The open Field test for measuring locomotor activity and anxiety-like behavior, Methods Mol. Biol. (2019) 99–103, https://doi.org/10.1007/978-1-4939-8994-2_9.
[55] N. Villacampa, B. Almolda, A. Vilella, I.L. Campbell, B. González, B. Castellano, Astrocyte-targeted production of IL-10 induces changes in microglial reactivity and reduces motor neuron death after facial nerve axotomy: facial Nerve Axotomy in GFAP-IL-10 Transgenic Mice, Glia 63 (2015) 1166–1184, https://doi.org/10.1002/glia.22807.